

Computational Optics  
Christoph Pflaum, SS 2017

## Contents

<b>1</b>	<b>Introduction to Computational Optics</b>	<b>3</b>
<b>2</b>	<b>Basic Physical Equations</b>	<b>8</b>
2.1	Maxwell's Equations and Helmholtz's Equation . . . . .	8
2.2	Refraction Indices . . . . .	10
2.3	Time Periodic Solutions . . . . .	12
<b>3</b>	<b>Solving Maxwell's Equations</b>	<b>13</b>
3.1	Finite Difference Time Domain Discretization (FDTD) . . . . .	13
3.2	Stability of FDTD . . . . .	16
3.3	Implementation of the FDTD Method . . . . .	20
3.4	Simple Boundary Condition . . . . .	21
3.5	PML Boundary Condition . . . . .	22
3.6	Incoming Boundary Condition with PML . . . . .	24
3.7	Calculation of Time Periodic Solutions . . . . .	25
3.8	Stable Iteration Method for Negative Permittivity . . . . .	28
<b>4</b>	<b>Beam Propagation</b>	<b>29</b>
4.1	Paraxial Approximation . . . . .	29
4.2	Beam Propagation Method BPM . . . . .	30
<b>5</b>	<b>Basic Properties of a Laser</b>	<b>30</b>
5.1	Elements of a Laser . . . . .	30
5.2	Atomic Energy Levels, Spontaneous Emission and Stimulated Transition . . . . .	32
5.3	Pumping Process and Population Inversion . . . . .	35
5.4	Example of Scalar Rate Equations . . . . .	36
5.5	Laser Amplification and Oscillation Condition . . . . .	38
<b>6</b>	<b>Numerical Discretization of a Scalar Rate Equation</b>	<b>40</b>

<b>7</b>	<b>Mode-Analysis</b>	<b>42</b>
7.1	Gauss Mode Analysis . . . . .	42
7.1.1	The Lowest Order Gauss-Mode . . . . .	42
7.1.2	Gauss Mode in an Aperture . . . . .	46
7.1.3	Ray Optics and ABCD Matrix . . . . .	48
7.1.4	ABCD Matrix of free space . . . . .	49
7.1.5	ABCD Matrix of a lense . . . . .	50
7.1.6	ABCD Matrix of a Mirror . . . . .	54
7.1.7	Other ABCD Matrices . . . . .	54
7.1.8	Ray (or Beam) Matrix of the Resonator . . . . .	55
7.1.9	Exact Solution in a Gaussian “Duct” . . . . .	57
7.1.10	The Guoy Phase Shift . . . . .	57
7.1.11	High Order Modes . . . . .	58
7.1.12	Thermal Lensing . . . . .	59
7.2	Iteration Method of Fox and Li . . . . .	60
<b>8</b>	<b>Finite Element Discretization of Optical Waves in Semicon-</b>	
	<b>ductor Laser Resonators</b>	<b>61</b>
8.1	Construction of Semiconductor Lasers . . . . .	61
8.2	Transfer Matrix Method . . . . .	62

# 1 Introduction to Computational Optics

## Application of Computational Optics

- propagation of light in glass fibers
- thin film solar cell simulation
- laser simulation
- optical lithography
- laser matter interaction
- ...

## Simulation Methods in Computational Optics

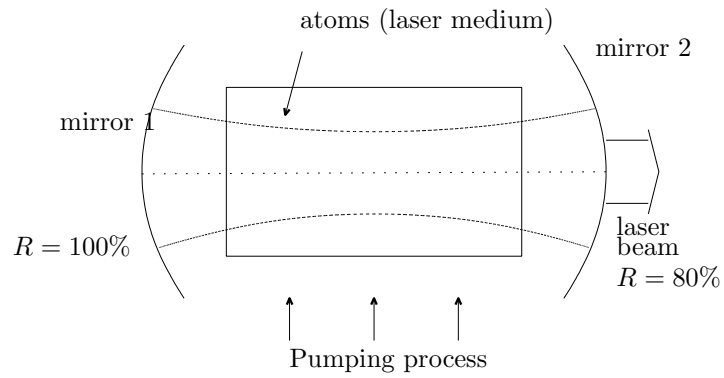
- Finite Difference Time Domain Method
- Beam Propagation Method
- Rate Equation
- Finite Element Method
- ...

## Application to

- wave propagation in solar cell simulation
- simulation of lasers (solid state lasers)
- ...

## Diode Pumped Solid-State Lasers

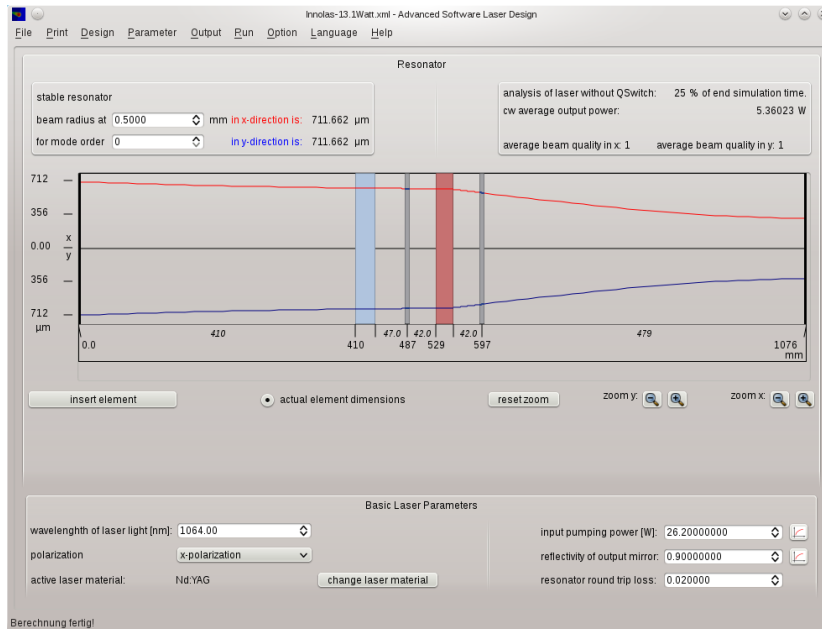
Let us describe the basic concept of a diode pumped solid-state laser.



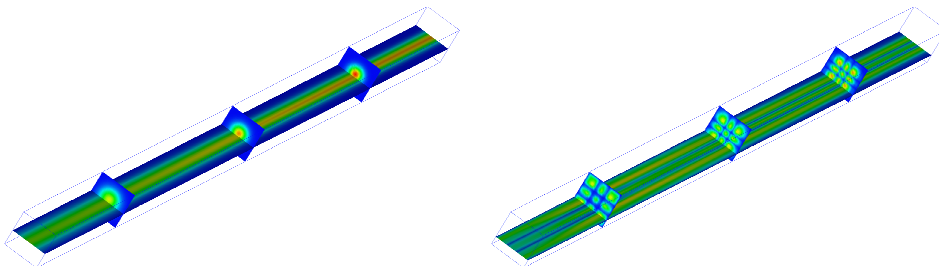
- A pumping light (diode light) pumps energy in a laser crystal. This means that electrons are pumped from a lower energy level to a higher energy level.
- A light (laser light) is gained inside of the crystal.

The pumping light heats the laser crystal. This leads to a thermal lensing effect inside the laser resonator.

The simulation program ASLD is a program for simulating diode pumped solid state lasers:



Our aim is to perform 3-dimensional simulations of optical waves in lasers:



### Simulation of Thin Film Solar Cells

Thin film solar cells are a new generation of solar cells.

- The thickness of these cells is only a few micrometers.
- The manufacturing cost are very low.
- But: The efficiency of thin film solar cells is much lower than the efficiency of standard solar cells.

Research institutes working on thin film solar cells:

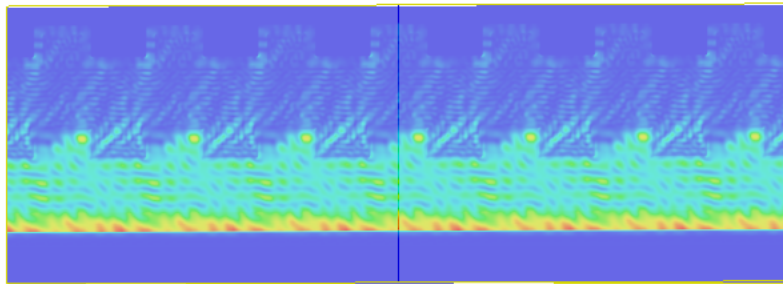
- National Renewable Energy Laboratory (NREL, Golden Colorado)
- Institute of Energy Research (Jülich, Germany)
- ...

#### Light in a Thin Film Solar Cell

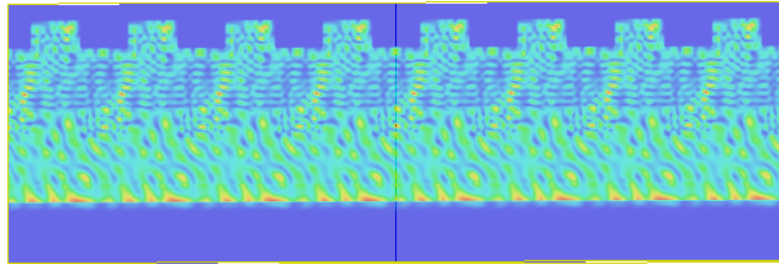
To optimize the efficiency of thin film solar cells it is necessary to simulate the optical properties of these cells. To this end, it is necessary to solve Maxwell's equations for plane waves which incident the top the cells:

Incident angle of optical wave:  $60^\circ$

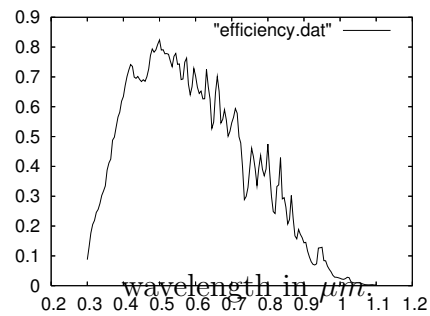
wavelength  $\lambda = 505nm$ :



wavelength  $\lambda = 700nm$ :



Only a certain fraction of the light is absorbed in the silicon part of a solar cell. The rest of the light is reflected. The following picture shows the optical efficiency of a thin film solar cell calculated by the FDTD method. The efficiency depends on the wavelength of the incident wave.



$$\text{total optical efficiency} = \text{optical efficiency} * \text{power of sun}$$

## 2 Basic Physical Equations

### 2.1 Maxwell's Equations and Helmholtz's Equation

The physical variables of Maxwell's equations are the 3D-vectors (see [?]):

$$\begin{aligned}\vec{E} &= \text{electric field intensity (volts / meter)} \\ \vec{D} &= \text{electric field density (coulombs / meter}^2\text{)} \\ \vec{H} &= \text{magnetic field intensity (amperes / meter)} \\ \vec{B} &= \text{magnetic field density (webers / meter}^2\text{)} \\ \vec{J} &= \text{electric current density (amperes / meter}^2\text{)}\end{aligned}$$

the scalar value

$$\rho = \text{electric charge density (coulombs / meter}^3\text{)}$$

and the material parameter

$$\epsilon = \text{permittivity (farads/meter)}$$

$$\mu = \text{permeability (henry/meter)}$$

$$\begin{aligned}\nabla \times \vec{E} &= -\frac{\partial \vec{B}}{\partial t} && \text{Faraday's law} \\ \nabla \times \vec{H} &= \frac{\partial \vec{D}}{\partial t} + \vec{J} && \text{Maxwell-Ampere law} \\ \nabla \cdot \vec{D} &= \rho && \text{Gauss's law} \\ \nabla \cdot \vec{B} &= 0 && \text{Gauss's law - magnetic} \\ \nabla \cdot \vec{J} &= -\frac{\partial \rho}{\partial t} && \text{equation of continuity}\end{aligned}$$

and constitutive relations:

$$\vec{D} = \epsilon \vec{E}, \quad \vec{B} = \mu \vec{H}, \quad \vec{J} = \sigma \vec{E}$$

In computational optics common assumptions are

- $\mu$  is constant,
- $\rho = 0$ , and
- $J = \sigma \vec{E}$ ,  
where  $\sigma$  is the electrical conductivity (siemens / meter).



By these assumptions, we get

$$\begin{aligned}\nabla \times \vec{E} &= -\mu \frac{\partial \vec{H}}{\partial t}, \\ \nabla \times \vec{H} &= \epsilon \frac{\partial \vec{E}}{\partial t} + \sigma \vec{E}, \\ \nabla \cdot (\epsilon \vec{E}) &= 0, \\ \nabla \cdot \vec{H} &= 0.\end{aligned}$$

**Example 1** (E-polarization plane wave:). Assume that  $\epsilon$  and  $\mu$  are constant and that  $\sigma = 0$ . Let  $\omega$  be a given frequency. Then,

$$\begin{aligned}E(t, (x, y, z)) &= \exp(i(\omega t - ky)) E_0 (0, 0, 1), \\ H(t, (x, y, z)) &= \exp(i(\omega t - ky)) H_0 (1, 0, 0),\end{aligned}$$

where

$$k = \sqrt{\mu\epsilon}\omega, \quad H_0 = \frac{k}{\mu\omega} E_0 = \frac{\epsilon\omega}{k} E_0$$

is a solution of Maxwell's equations.

This plane wave is called *E-polarization plane wave* in the  $(x, y)$ -plane.

Since  $\mu$  is constant, we get from Maxwell's equations:

$$\begin{aligned}\nabla \times \nabla \times \vec{E} &= -\mu \frac{\partial}{\partial t} \nabla \times \vec{H} \\ &= -\mu \frac{\partial}{\partial t} \left( \epsilon \frac{\partial \vec{E}}{\partial t} + \sigma \vec{E} \right) \\ &= -\mu\epsilon \frac{\partial^2 \vec{E}}{\partial t^2} - \mu\sigma \frac{\partial \vec{E}}{\partial t}.\end{aligned}$$

Thus, we get the vector Helmholtz equation:

$$\nabla \times \nabla \times \vec{E} = -\mu\epsilon \frac{\partial^2 \vec{E}}{\partial t^2} - \mu\sigma \frac{\partial \vec{E}}{\partial t}.$$

Let us assume the  $\epsilon$  is constant. (But, often  $\epsilon$  is not constant!) Then, we get

$$\epsilon \nabla \cdot \vec{E} = \nabla \cdot \vec{D} = \rho = 0.$$

This implies

$$\nabla(\nabla \cdot \vec{E}) = 0. \quad (1)$$

Then, we get

$$\nabla \times \nabla \times \vec{E} = \nabla(\nabla \cdot \vec{E}) - \Delta \vec{E} = -\Delta \vec{E}$$

Now, the vector-Helmholtz equation

$$\nabla \times \nabla \times \vec{E} = -\mu\epsilon \frac{\partial^2 \vec{E}}{\partial t^2} - \mu\sigma \frac{\partial \vec{E}}{\partial t}.$$

and the assumption (1) imply

$$-\Delta \vec{E} = -\mu\epsilon \frac{\partial^2 \vec{E}}{\partial t^2} - \mu\sigma \frac{\partial \vec{E}}{\partial t}.$$

Let us consider one component  $e_z E(x, y, z)$  of this equation. Then, we get the scalar Helmholtz equation:

$$-\Delta E = -\mu\epsilon \frac{\partial^2 E}{\partial t^2} - \mu\sigma \frac{\partial E}{\partial t}. \quad (2)$$

**Example 2** (Plane wave). Assume that  $\epsilon$  and  $\mu$  are constant and  $\sigma = 0$ . Let  $\omega$  be a given frequency. Then,

$$E(t, (x, y, z)) = \exp(i(\omega t - ky)) E_0$$

where

$$k = \sqrt{\mu\epsilon}\omega,$$

is a solution of the scalar Helmholtz equation.

## 2.2 Refraction Indices

In vacuum, it is

$$\begin{aligned} \epsilon &:= \epsilon_0 = 8.854 \cdot 10^{-12} \text{ farads/meter}, \\ \mu &:= \mu_0 = 4\pi \cdot 10^{-7} \text{ henrys/meter}, \\ c &:= \sqrt{\frac{1}{\epsilon_0\mu_0}}, \end{aligned}$$

where  $c$  is the velocity of light.

By Example 2, we see that in vacuum  $k = \frac{\omega}{c}$  and that  $\lambda = \frac{2\pi}{k}$  is the wavelength in vacuum. Thus, the wavelength in vacuum is

$$\lambda = \frac{2\pi c}{\omega}.$$

In a general material let us define

$$\begin{aligned}\epsilon_r &= \epsilon/\epsilon_0, \\ \mu_r &= \mu/\mu_0.\end{aligned}$$

In computational optics  $\mu_r = 1$ .

The complex refractive index

$$n_C = n_R - in_I$$

is defined such that the wave

$$E = E_0 \cos(\omega(t - n_R y/c)) e^{-\omega n_I y/c} \quad (3)$$

is a wave traveling through a material with complex refractive index  $n_C = n_R - in_I$  (see Hecht page 198).

This definition is based on two experiments.

**Experiment 1** (Absorption). *Send a wave with frequency  $\omega$  through a material with thickness  $d$ . Let  $\Delta$  be the measured damping of  $|E|$  while the wave travels through the material. Then, define  $n_I$  by:*

$$\Delta = e^{-\omega n_I d/c}.$$

**Experiment 2** (Local Wavelength). *Send a wave with frequency  $\omega$  through a material. Let  $\lambda_{\text{loc}}$  be the measured wavelength inside the material. Then, define  $n_R$  by:*

$$\omega n_R \lambda_{\text{loc}}/c = 2\pi.$$

**Formula 1.**

$$\begin{aligned}\epsilon_r &= n_R^2 - n_I^2 \\ \sigma &= 4\pi \sqrt{\frac{\epsilon_0}{\mu_0}} \frac{n_R n_I}{\lambda},\end{aligned}$$

where  $\lambda$  is the wavelength in vacuum.

*Proof.* Let us insert the ansatz (3) in the wave equation (2). This means

$$E = E_0 \cos(\omega(t - n_R y/c)) e^{-\omega n_I y/c}$$

in

$$\Delta E = \mu_0 \epsilon \frac{\partial^2 E}{\partial t^2} + \mu_0 \sigma \frac{\partial E}{\partial t}.$$

Comparing the cosines terms, we get

$$-\frac{n_R^2}{c^2} \omega^2 + \omega^2 \frac{n_I^2}{c^2} = -\omega^2 \mu_0 \epsilon.$$

Using  $c := \sqrt{\frac{1}{\epsilon_0 \mu_0}}$  this implies

$$\epsilon_r = n_R^2 - n_I^2.$$

Comparing the sinus terms, we get

$$-2\omega \frac{n_R}{c} \omega \frac{n_I}{c} = -\omega \mu_0 \sigma.$$

Using the equation

$$\omega = \frac{2\pi c}{\lambda},$$

this implies

$$\sigma = \frac{4\pi}{c\mu_0} \frac{n_R n_I}{\lambda} = 4\pi \sqrt{\frac{\epsilon_0}{\mu_0}} \frac{n_R n_I}{\lambda}.$$

□

### 2.3 Time Periodic Solutions

Let us assume that  $E$  is time periodic. This means:

$$E(x, y, z, t) = \exp(i\omega t) E(x, y, z).$$

Inserting in the scalar Helmholtz equation, leads to

$$-\Delta E - k^2 E = 0,$$

where  $k^2 = \mu \epsilon \omega^2$ .

This is the Helmholtz equation for time periodic solutions.

### 3 Solving Maxwell's Equations

#### 3.1 Finite Difference Time Domain Discretization (FDTD)

Lets first define a staggered grid on the 1-dimensional interval  $[0, L]$ , and let  $0 = x_0 < x_1, \dots, x_N = L$  be a finite sequence of grid points. Now, lets denote

$$\Omega_c := \{x_0, x_1, \dots, x_N\}$$

to be the set of corner points. The staggered grid or dual grid corresponding to  $\Omega_c$  is

$$\Omega_s := \{s_0, s_1, \dots, s_{N-1}\}$$

where

$$s_i = \frac{1}{2}(x_i + x_{i+1}) \quad \text{for } i = 0, \dots, N-1.$$

**Example 3** (Uniform Staggered Grid in 1D). *Let  $x_i = i * \frac{L}{N}$ ,  $i = 0, \dots, N$  be the uniform grid of mesh size  $h = \frac{L}{N}$ . Then, the corresponding staggered grid is  $s_i = (i - 0.5) * \frac{L}{N}$ ,  $i = 1, \dots, N$  (see Figure 1).*

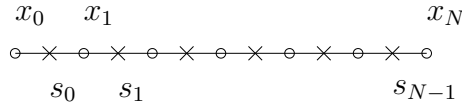


Figure 1: Staggered grid in 1D.

For the definition of a staggered grid in three dimensions, lets restrict ourselves to the rectangular domain

$$\Omega = [0, L_x] \times [0, L_y] \times [0, L_z].$$

Furthermore, lets assume that the 1-dimensional intervals  $[0, L_x]$ ,  $[0, L_y]$ , and  $[0, L_z]$  are discretized by the 1-dimensional grids

$$\begin{aligned} \Omega_c^x &:= \{x_0, x_1, \dots, x_{N_x}\}, & \Omega_c^y &:= \{y_0, y_1, \dots, y_{N_y}\}, & \text{and} \\ \Omega_c^z &:= \{z_0, z_1, \dots, z_{N_z}\}. \end{aligned}$$

Then, 8 types of grids exist in  $\Omega$ , which can be composed of these 1-dimensional grids. These grids are

$$\Omega_{t_x, t_y, t_z} = \Omega_{t_x}^x \times \Omega_{t_y}^y \times \Omega_{t_z}^z,$$

where  $(t_x, t_y, t_z) \in \{c, s\}^3$ .

**Example 4.**

- $\Omega_{ccs}$ ,  $\Omega_{csc}$ , and  $\Omega_{scc}$ , are the staggered grids located at the edges of a discretization cell.
- $\Omega_{css}$ ,  $\Omega_{scs}$ , and  $\Omega_{ssc}$ , are the staggered grids located at the faces of a discretization cell.

See Figure 2.

The grids  $\Omega_{t_x, t_y, t_z}$  are grids on a simple rectangular domain  $\Omega = [0, L_x] \times [0, L_y] \times [0, L_z]$ . Obviously a generalization to other rectangular domain is a simple task. However, a generalization to curvilinear domains or block-structured grids requires certain modifications. Handling curvilinear domains correctly, is mainly a discretizations problem and not a data structure problem. By introducing coordinate functions  $X, Y, Z$  one can implement every discretization on structured grids and curvilinear domains. However, block-structured grids might lead to complications, if the composition of the blocks changes the x-,y-,z-orientation of the blocks. In this case, one should introduce a grid on edges and a grid on faces. Furthermore, we recommend edge elements as a discretization on such grids. This will increase the complexity and the storage requirement of these discretizations. Therefore, let us restrict ourselves to rectangular domains.

Let us consider Maxwell's equations in 3D in the following form:

$$\begin{aligned} \epsilon \frac{\partial \vec{E}}{\partial t} &= \nabla \times \vec{H} - \sigma \vec{E}, \\ \mu \frac{\partial \vec{H}}{\partial t} &= -\nabla \times \vec{E} - \sigma^* \vec{H}, \\ \nabla \cdot (\epsilon \vec{E}) &= 0, \\ \nabla \cdot \vec{H} &= 0. \end{aligned}$$

The Yee algorithms discretize  $\vec{E}$  and  $\vec{H}$  on the staggered grids. For reasons of simplicity, lets restrict ourselves to a uniform staggered grids:

$$\begin{aligned} \Omega_{t_x, t_y, t_z} & \text{ in space with mesh sizes } h_x = \frac{L_x}{N_x}, h_y = \frac{L_y}{N_y}, h_z = \frac{L_z}{N_z} \text{ and} \\ \Omega_t^\tau & \text{ in time with time step } \tau. \end{aligned}$$

The fields  $\vec{E}$  and  $\vec{H}$  are discretized at the faces and edges of the mesh cells

$$E_x|_p^t, \quad p \in \Omega_{css}, \quad E_y|_p^t, \quad p \in \Omega_{scs}, \quad E_z|_p^t, \quad p \in \Omega_{ssc}, \quad \forall t \in \Omega_s^\tau,$$

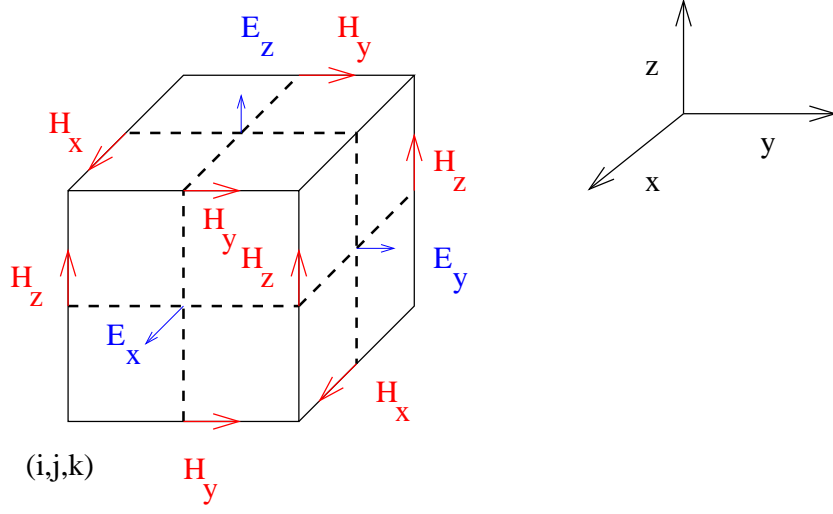


Figure 2: Staggered grid in 3D.

$$H_x|_p, \quad p \in \Omega_{scc}, \quad H_y|_p, \quad p \in \Omega_{csc}, \quad H_z|_p, \quad p \in \Omega_{ccs}, \quad \forall t \in \Omega_c^\tau.$$

The finite difference time domain method (FDTD) discretizes the first component of Maxwell's equations as follows:

$$\begin{aligned} \frac{E_x|_M^{t+\frac{\tau}{2}} - E_x|_M^{t-\frac{\tau}{2}}}{\tau} &= \frac{1}{\epsilon} \left( \frac{H_z|_N^t - H_z|_S^t}{h_y} - \frac{H_y|_T^t - H_y|_D^t}{h_z} \right. \\ &\quad \left. - \sigma(\rho E_x|_M^{t+\frac{\tau}{2}} + (1-\rho)E_x|_M^{t-\frac{\tau}{2}}) \right) \\ &\quad \forall M \in \Omega_{css}, \quad t \in \Omega_c^\tau. \end{aligned}$$

where

$$\begin{aligned} W &= M + e_x \frac{h_x}{2}, & E &= M - e_x \frac{h_x}{2}, \\ N &= M + e_y \frac{h_y}{2}, & S &= M - e_y \frac{h_y}{2}, \\ T &= M + e_z \frac{h_z}{2}, & D &= M - e_z \frac{h_z}{2}. \end{aligned}$$

and  $\rho \in [0, 1]$ .

This leads to the update formula

$$\begin{aligned} E_x|_M^{t+\frac{\tau}{2}} &= \left( E_x|_M^{t-\frac{\tau}{2}} + \frac{\tau}{\epsilon} \left( \frac{H_z|_N^t - H_z|_S^t}{h_y} - \frac{H_y|_T^t - H_y|_D^t}{h_z} \right. \right. \\ &\quad \left. \left. - \sigma(1-\rho)E_x|_M^{t-\frac{\tau}{2}} \right) \right) \frac{1}{1 + \frac{\sigma\rho\tau}{\epsilon}} \end{aligned}$$

$$\forall M \in \Omega_{css}, t \in \Omega_c^T.$$

The other Maxwell's equations are discretized analogously.

In case of  $\sigma = 0$ , one obtains the update formula

$$E_x|_M^{t+\frac{\tau}{2}} = E_x|_M^{t-\frac{\tau}{2}} + \frac{\tau}{\epsilon} \left( \frac{H_z|_N^t - H_z|_S^t}{h_y} - \frac{H_y|_T^t - H_y|_D^t}{h_z} \right) \quad (4)$$

$$\forall M \in \Omega_{css}, t \in \Omega_c^T.$$

The other Maxwell's equations are discretized analogously.

### 3.2 Stability of FDTD

The Finite Difference Time Domain Method (FDTD) is an explicit method for the discretization of Maxwell's equations. Therefore, the time step has to be small enough and the coefficients have to satisfy certain conditions to obtain convergence.

#### Stability of Time Stepping

**Definition 1.** *The finite difference time domain method is stable if the solution is bounded for any initial condition and periodic boundary conditions.*

**Theorem 1** (CFL-Condition). *Assume that  $\sigma \geq 0$  and  $\epsilon > 0$ . Let*

$$\xi = \frac{1}{\sqrt{|\mu\epsilon|}} \tau \sqrt{\frac{1}{h_x^2} + \frac{1}{h_y^2} + \frac{1}{h_z^2}}.$$

*The finite difference time domain method is stable if*

$$\xi < 1.$$

Let us prove this Theorem.

Let us consider the FDTD discretization in the short form for  $\vec{J}_{h,\tau} = 0$  and  $\vec{M}_{h,\tau} = 0$  and  $\mu = 1$  and  $\epsilon = 1$  :

$$\begin{aligned} \partial_\tau^1 \vec{H}_{h,\tau} &= -\nabla_h \times \vec{E}_{h,\tau} \quad \text{at time points } n + \frac{1}{2}, \\ \partial_\tau^1 \vec{E}_{h,\tau} &= \nabla_h \times \vec{H}_{h,\tau} \quad \text{at time points } n. \end{aligned}$$

Now, the abbreviation

$$\vec{V}_{h,\tau} = \vec{H}_{h,\tau} + j\vec{E}_{h,\tau}$$



leads to

$$\partial_\tau^1 \vec{V}_{h,\tau} = j \nabla_h \times \vec{V}_{h,\tau}$$

Observe, that  $\vec{V}_{h,\tau}$  is a vector defined at all edges and faces of each cell and which is defined at all time points  $t \frac{1}{2}n$ , where  $n \in \mathbb{N}$ . To this end set  $\vec{H}_{h,\tau}$  and  $\vec{E}_{h,\tau}$  to be zero at all points, where these vectors originally are not defined.

Now, we obtain the following lemma.

**Lemma 1.** *The FDTD method is stable, if the solution  $\vec{H}_{h,\tau}, \vec{E}_{h,\tau}$  is bounded for  $t \rightarrow \infty$ .*

Let us analyze

$$\partial_\tau^1 \vec{V}_{h,\tau} = j \nabla_h \times \vec{V}_{h,\tau}.$$

By Fourier analysis, we see that it is enough to analyze the behavior of the solutions with periodic initial condition:

$$\vec{V}_{h,\tau}(0, x, y, z) = \vec{V}_0 e^{j(-k_x x - k_y y - k_z z)}. \quad (5)$$

The FDTD method is stable, if  $\vec{V}_{h,\tau}$  has the form

$$\vec{V}_{h,\tau}(t, x, y, z) = \vec{V}_0 e^{j(\omega t - k_x x - k_y y - k_z z)}$$

for every edge point, face point, and every time step  $t \frac{1}{2}n$ . Observe, that a Fourier decomposition with periodic functions as in the ansatz (5) spans the whole space of possible initial conditions, since every unknown of the vectors  $\vec{H}_{h,\tau}$  and  $\vec{E}_{h,\tau}$  is located at a different spatial point.

The abbreviation  $\vec{V}_0 = (V_x, V_y, V_z)^T$  leads to

$$\begin{aligned} j \nabla_h \times \vec{V}_{h,\tau} &= \det \begin{pmatrix} e_x & \partial_{h_x,x}^1 & V_x \\ e_y & \partial_{h_y,y}^1 & V_y \\ e_z & \partial_{h_z,z}^1 & V_z \end{pmatrix} e^{j(\omega t - k_x x - k_y y - k_z z)} \\ &= j \det \begin{pmatrix} e_x & \frac{1}{h_x} \sin\left(\frac{k_x h_x}{2}\right) & V_x \\ e_y & \frac{1}{h_y} \sin\left(\frac{k_y h_y}{2}\right) & V_y \\ e_z & \frac{1}{h_z} \sin\left(\frac{k_z h_z}{2}\right) & V_z \end{pmatrix} e^{j(\omega t - k_x x - k_y y - k_z z)} = \\ \partial_\tau^1 \vec{V}_{h,\tau} &= \partial_\tau^1 \begin{pmatrix} V_x \\ V_y \\ V_z \end{pmatrix} e^{j(\omega t - k_x x - k_y y - k_z z)} \\ &= \frac{1}{\tau} \sin\left(\frac{\omega \tau}{2}\right) \begin{pmatrix} V_x \\ V_y \\ V_z \end{pmatrix} e^{j(\omega t - k_x x - k_y y - k_z z)} \end{aligned}$$

This is a linear equation system with unknowns  $V_x$ ,  $V_y$ , and  $V_z$ .

The equation system has a unique solution if and only if

$$\begin{aligned}
0 &= \det \begin{pmatrix} j\frac{1}{\tau} \sin(\frac{\omega\tau}{2}) & \frac{1}{h_z} \sin(\frac{k_z h_z}{2}) & -\frac{1}{h_y} \sin(\frac{k_y h_y}{2}) \\ \frac{1}{h_z} \sin(\frac{k_z h_z}{2}) & j\frac{1}{\tau} \sin(\frac{\omega\tau}{2}) & -\frac{1}{h_x} \sin(\frac{k_x h_x}{2}) \\ -\frac{1}{h_y} \sin(\frac{k_y h_y}{2}) & +\frac{1}{h_x} \sin(\frac{k_x h_x}{2}) & j\frac{1}{\tau} \sin(\frac{\omega\tau}{2}) \end{pmatrix} \\
&= \left( \left( \frac{1}{h_x} \sin(\frac{k_x h_x}{2}) \right)^2 + \left( \frac{1}{h_y} \sin(\frac{k_y h_y}{2}) \right)^2 + \left( \frac{1}{h_z} \sin(\frac{k_z h_z}{2}) \right)^2 \right. \\
&\quad \left. - \left( \frac{1}{\tau} \sin(\frac{\omega\tau}{2}) \right)^2 \right) j\frac{1}{\tau} \sin(\frac{\omega\tau}{2})
\end{aligned}$$

. This is equivalent to the *stability equation*:

$$\left( \frac{1}{h_x} \sin(\frac{k_x h_x}{2}) \right)^2 + \left( \frac{1}{h_y} \sin(\frac{k_y h_y}{2}) \right)^2 + \left( \frac{1}{h_z} \sin(\frac{k_z h_z}{2}) \right)^2 = \left( \frac{1}{\tau} \sin(\frac{\omega\tau}{2}) \right)^2$$

The *stability equation* has a solution  $\omega$  for every  $k_x, k_y, k_z$ , if

$$\tau \sqrt{\frac{1}{h_x^2} + \frac{1}{h_y^2} + \frac{1}{h_z^2}} < 1.$$

A renormalization of this stability condition shows

$$\tau < c^{-1} \left( \frac{1}{h_x^2} + \frac{1}{h_y^2} + \frac{1}{h_z^2} \right)^{-\frac{1}{2}}.$$

where  $c$  is the velocity of the wave.

Stability of Absorption Term

Let us recall the update formula:

$$\begin{aligned}
\frac{E_x|_M^{t+\frac{\tau}{2}} - E_x|_M^{t-\frac{\tau}{2}}}{\tau} &= \frac{1}{\epsilon} \left( \frac{H_z|_N^t - H_z|_S^t}{h_y} - \frac{H_y|_T^t - H_y|_D^t}{h_z} \right. \\
&\quad \left. - \sigma(\rho E_x|_M^{t+\frac{\tau}{2}} + (1-\rho)E_x|_M^{t-\frac{\tau}{2}}) \right)
\end{aligned}$$

Then, one obtains the following discretizations

- $\rho = 0$ : explicit discretization

- $\rho = 1$ : implicit discretization

To analyze the stability, of this discretizations, we consider the case that

$$0 = \frac{H_z|_N^t - H_z|_S^t}{h_y} - \frac{H_y|_T^t - H_y|_D^t}{h_z}.$$

Then, one obtains the following update formula:

$$E_x|_M^{t+\frac{\tau}{2}} = E_x|_M^{t-\frac{\tau}{2}} \frac{1 - \frac{\tau\sigma(1-\rho)}{\epsilon}}{1 + \frac{\sigma\rho\tau}{\epsilon}}.$$

Stability is obtained if

$$\left| \frac{1 - \frac{\tau\sigma(1-\rho)}{\epsilon}}{1 + \frac{\sigma\rho\tau}{\epsilon}} \right| \leq 1.$$

This implies:

- $\rho = 0$ : stability if  $|\frac{\tau\sigma}{\epsilon}| < 1$ .
- $\rho = 1$ : stability if  $\text{sign}(\sigma\epsilon) = 1$ .

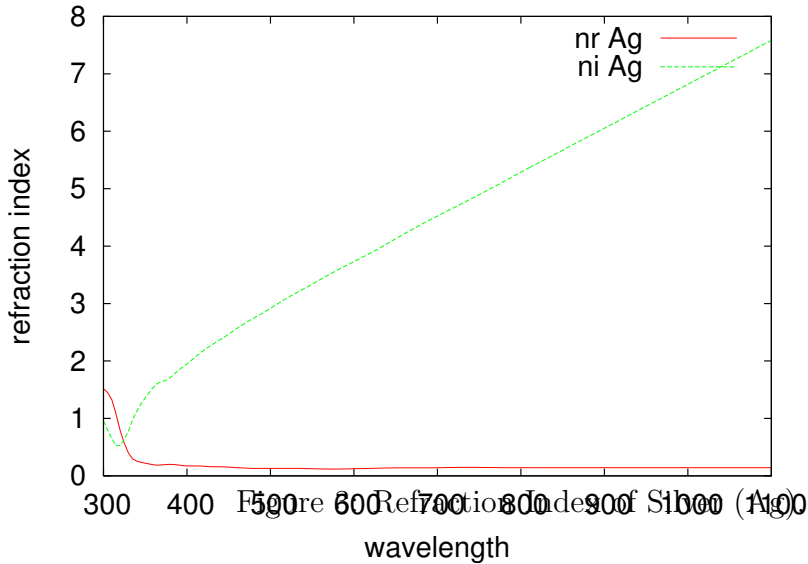
Difficulty:  $\text{sign}(\sigma\epsilon) = -1$ . This happens in case of materials with negative permittivity index.

**Definition 2.** *A material has negative permittivity index if  $\epsilon_r < 0$ .*

**Example 5** (Silver). *The refraction indices of silver (Ag) at wavelength  $\lambda = 500\text{nm}$  are:  $n_R = 0.13$  and  $n_I = 2.9637$ . This implies*

$$\epsilon_r = n_R^2 - n_I^2 = -8.78796929.$$

Figure 3 depicts the refraction indices of silver (Ag). These data imply that silver has a negative permittivity for  $\lambda \geq 325\text{nm}$ . In Section 3.7, we describe a stable discretization for time periodic solutions.



### 3.3 Implementation of the FDTD Method

To implement algorithms on staggered grids let us define a class variable which represents a vector  $(v_p)_{p \in \Omega_{t_x, t_y, t_z}}$ :

```
enum stag_typ { not_stag, stag };
```

```
template <stag_typ tx, stag_typ ty, stag_typ tz>
class Variable {
    Variable(double L, int N_points);
    ...
};
```

Here  $L$  is the size of the computational domain  $\Omega = [0, L]^3$  and  $N\_points$  is the number of grid cells in  $x$ -,  $y$ -, and  $z$ -direction.

Furthermore, let us assume that we can implement shift operators  $N, S, \dots$  which evaluate a vector at its corresponding shifted indices. Then, a natural implementation of the update formula 4 is

```
double tau, epsilon, hy, hz;
double L = 2.0;
```

```

int    Np = 200;
Variable<not_stag,stag,stag> Ex(L,Np);
...
Variable<not_stag,not_stag,stag> Hz(L,Np);
Variable<not_stag,stag,not_stag> Hy(L,Np);
...
Ex = Ex + tau / epsilon
      ( ( N(Hz) - S(Hz) ) / hy -
        ( T(Hy) - D(Hy) ) / hz );

```

By expression templates, one can implement the above update formula in an efficient way.

By the template parameter, one can forbid mathematically incorrect expressions like

$$\mathbf{Ex} = \mathbf{Ex} + (\mathbf{T}(\mathbf{Hz}) - \mathbf{D}(\mathbf{Hz})); \quad (6)$$

This expressions is mathematically incorrect, since data of the vector  $\mathbf{Ex}$  is located on the grid  $\Omega_{c,s,s}$  and the data of  $\mathbf{T}(\mathbf{Hz})$  is located on the grid  $\Omega_{c,c,c}$ . Therefore, no arithmetic operations can be performed for Equation (6). However,

$$\mathbf{Ex} = \mathbf{Ex} + (\mathbf{N}(\mathbf{Hz}) - \mathbf{S}(\mathbf{Hz})); \quad (7)$$

is a correct expression with staggered grid data.

### 3.4 Simple Boundary Condition

There exist three simple boundary conditions:

- periodic boundary conditions
- strict incoming boundary condition
- reflection boundary condition

Periodic Boundary Condition Let  $\Gamma_E$  and  $\Gamma_W$  be the east and west boundary face of the computational domain. The periodic boundary condition is:

$$\begin{aligned} E|_{\Gamma_E} &= E|_{\Gamma_W} \\ H|_{\Gamma_E} &= H|_{\Gamma_W}. \end{aligned}$$

Reflection Boundary Condition Let  $\Gamma_{\text{reflect}}$  be part of the boundary. Reflection at  $\Gamma_{\text{reflect}}$  can be modelled by

$$E|_{\Gamma_{\text{reflect}}} = 0.$$

Strict Incoming Boundary Condition Let

- $\Gamma$  be a flat part of the boundary,
- $\vec{n}$  the inner normal vector, and
- $\vec{t}_a$  and  $\vec{t}_b$  two orthonormal vectors orthogonal to  $\vec{n}$ .

Setting

$$\begin{aligned} E(t, \vec{x}) &= \exp(i(\omega t - k\vec{n} \circ \vec{x})) E_0 \vec{t}_a, \\ H(t, \vec{x}) &= \exp(i(\omega t - k\vec{n} \circ \vec{x})) H_0 \vec{t}_b \end{aligned}$$

at  $\Gamma$ , where  $H_0 = \frac{k}{\mu\omega} E_0$ ,

leads to an incoming wave condition.

Since all data are located at a staggered grid often only one of the above equations is needed at the boundary  $\Gamma$ .

### 3.5 PML Boundary Condition

It is difficult to define a boundary condition without reflections. These are not Neumann boundary conditions!

Let assume that a plane wave ( $H_z, E_y$ ) travels in x-direction (see Figure 4).

The wave is absorbed without reflections, if one chooses  $\sigma^* = \sigma_{\epsilon}^{\mu} > 0$ .

Absorbing boundary conditions have to be implemented by an extension of the computational domain (see Figure 5). This extension domain is called PML (Perfect Matched Boundary Layer).

In this domain the wave has to be absorbed without reflections. The size of the domain should be roughly 2 wavelength.

However, just choosing  $\sigma^* = \sigma_{\epsilon}^{\mu}$  in the extended domain leads to reflection for oblique incident waves at the absorbing boundary. Therefore, one has to split the fields  $\vec{H}$  and  $\vec{E}$ .

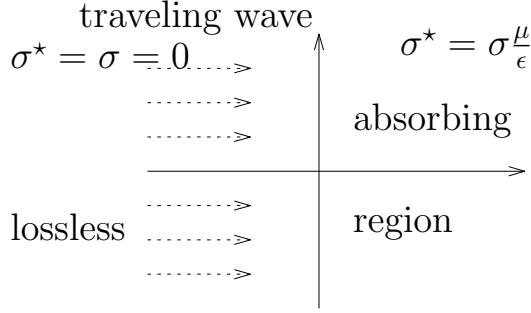


Figure 4: Plane Wave Incident Upon a Lossy Half-Space.  
periodic boundary condition

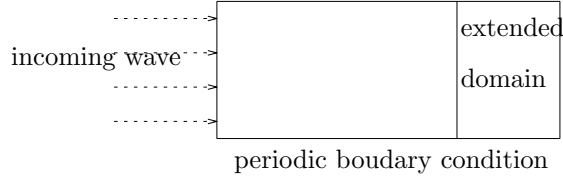


Figure 5: Extension of the Computational Domain.

To explain this, consider the update formula

$$E_y|_M^{t+\frac{\tau}{2}} = E_y|_M^{t-\frac{\tau}{2}} + \frac{\tau}{\epsilon} \left( \frac{H_x|_T^t - H_x|_D^t}{h_z} - \frac{H_z|_E^t - H_z|_W^t}{h_x} \right)$$

This formula can be split as follows

$$\begin{aligned} E_{yx}|_M^{t+\frac{\tau}{2}} &= E_{yx}|_M^{t-\frac{\tau}{2}} + \frac{\tau}{\epsilon} \left( \frac{H_{xy}|_T^t + H_{xz}|_T^t - H_{xy}|_D^t - H_{xz}|_D^t}{h_z} \right) \\ E_{yz}|_M^{t+\frac{\tau}{2}} &= E_{yz}|_M^{t-\frac{\tau}{2}} - \frac{\tau}{\epsilon} \left( \frac{H_{zx}|_E^t + H_{zy}|_E^t - H_{zx}|_W^t - H_{zy}|_W^t}{h_x} \right) \\ E_y &= E_{yx} + E_{yz} \\ H_x &= H_{xy} + H_{xz} \\ H_z &= H_{zx} + H_{zy}. \end{aligned}$$

The general update formula

$$\begin{aligned} E_y|_M^{t+\frac{\tau}{2}} &= \left( E_y|_M^{t-\frac{\tau}{2}} + \frac{\tau}{\epsilon} \left( \frac{H_x|_T^t - H_x|_D^t}{h_z} - \frac{H_z|_E^t - H_z|_W^t}{h_x} \right. \right. \\ &\quad \left. \left. - \sigma(1 - \rho)E_y|_M^{t-\frac{\tau}{2}} \right) \right) \frac{1}{1 + \frac{\sigma\rho\tau}{\epsilon}}. \end{aligned}$$

is split as follows:

$$E_{yx}|_M^{t+\frac{\tau}{2}} = \left( \dots - \sigma_z(1 - \rho) \left( E_{yx}|_M^{t-\frac{\tau}{2}} \right) \right) \frac{1}{1 + \frac{\sigma_z \rho \tau}{\epsilon}}$$

$$E_{yz}|_M^{t+\frac{\tau}{2}} = \left( \dots - \sigma_x(1 - \rho) \left( E_{yz}|_M^{t-\frac{\tau}{2}} \right) \right) \frac{1}{1 + \frac{\sigma_x \rho \tau}{\epsilon}}.$$

Inside the physical domain choose  $\sigma_x = \sigma_y = \sigma_z = \sigma$ .

In a PML region orthogonal to the x-direction, choose  $\sigma_x^* = \sigma_x \frac{\mu}{\epsilon} > 0$ .

In the PML region in Figure 5 choose  $\sigma_x^* = \sigma_x \frac{\mu}{\epsilon} > 0$ .

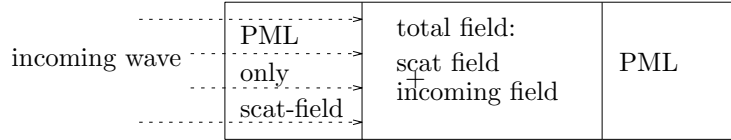
$\sigma_x$  can be chosen constant or quadratic increasing in the PML region.

### 3.6 Incoming Boundary Condition with PML

Consider an incoming wave  $(Ey, Hz)$  traveling in x-direction. To avoid reflections at the incoming boundary, we have to split the field in a scattered-wave field and a incoming-wave field.

$$\vec{E}^{total} = \vec{E}^{inc} + \vec{E}^{scat},$$

$$\vec{H}^{total} = \vec{H}^{inc} + \vec{H}^{scat}.$$



However, we store only one field as follows:

- PML-region: store only scattered-wave field.
- physical domain: store only total field.
- interface-region: store only total field. The interface-region is the interior boundary between the PML-region and the physical domain. The incoming wave has to be defined at this region.

Let us define three kind of subdomains of the computational domain:

- $\Gamma_{in}$ : incoming boundary; interface between physical domain and PML. Assume that we store the field component  $E_z$  at this interface.



- $\Gamma_{next}$ : next layer of grid points in the PML region parallel to  $\Gamma_{in}$ .
- $\Omega_{rest}$ : all other grid points.

Apply this formula at all points  $\Omega_{rest}$ :

$$E_y|_M^{t+\frac{\tau}{2}} = E_y|_M^{t-\frac{\tau}{2}} + \frac{\tau}{\epsilon} \left( \frac{H_x|_T^t - H_x|_D^t}{h_z} - \frac{H_z|_E^t - H_z|_W^t}{h_x} \right)$$

Let us assume a  $(Ey, Hz)$  incoming wave traveling in x-direction.

Apply this formula at all points  $\Gamma_{in}$ :

$$E_y|_M^{t+\frac{\tau}{2}} = E_y|_M^{t-\frac{\tau}{2}} + \frac{\tau}{\epsilon} \left( \frac{H_x|_T^t - H_x|_D^t}{h_z} - \frac{H_z|_E^t - (H_z|_W^t + H_z|_W^{t,inc})}{h_x} \right)$$

Apply this formula at all points  $\Gamma_{next}$ :

$$H_z|_M^{t+\frac{\tau}{2}} = H_z|_M^{t-\frac{\tau}{2}} - \frac{\tau}{\epsilon} \left( \frac{E_y|_E^t - (E_y|_W^t - E_y|_W^{t,inc})}{h_x} - \frac{E_x|_N^t - E_x|_S^t}{h_y} \right)$$

### 3.7 Calculation of Time Periodic Solutions

To describe the formulation, we assume the media is linear and isotropic. The finite difference frequency domain method is a discretization of Maxwell's equations for a time periodic source:

$$\begin{aligned} i\omega \hat{E} &= \frac{1}{\epsilon} \nabla \times \hat{H} - \frac{\sigma}{\epsilon} \hat{E}, \\ i\omega \hat{H} &= -\frac{1}{\mu} \nabla \times \hat{E} - \frac{\sigma^*}{\mu} \hat{H}, \end{aligned} \quad (8)$$

where we consider a source defined at the boundary of simulation domain.

Here, let us restrict ourselves to the domain  $\Omega = [0, L_x] \times [0, L_y] \times [0, L_z]$ . For reason of simplicity, we consider periodic boundary conditions in x- and y-direction, an incoming plane wave at the top face  $\Gamma_{top} = [0, L_x] \times [0, L_y] \times \{L_z\}$  described by

$$\begin{aligned} \hat{H}_x(p) &= H_0, \\ \hat{E}_y(p) &= E_0, \\ \hat{H}_y(p) = \hat{H}_z(p) = \hat{E}_x(p) = \hat{E}_z(p) &= 0, \end{aligned}$$

where  $H_0 = \sqrt{\frac{\epsilon}{\mu}} E_0$ ,  $p \in \Gamma_{top}$ .

To find a stable discretization of equation (8) with a suitable iterative solver, a common method is to apply the FDTD method and to use the time stepping as an iterative solver. Let us describe this approach in detail.

The time dependent Maxwell's equations that describes electromagnetic wave propagation in a linear, lossy media are

$$\frac{\partial \vec{E}}{\partial t} = \frac{1}{\epsilon} \nabla \times \vec{H} - \frac{\sigma}{\epsilon} \vec{E} \quad (9)$$

$$\frac{\partial \vec{H}}{\partial t} = -\frac{1}{\mu} \nabla \times \vec{E} - \frac{\sigma^*}{\mu} \vec{H}. \quad (10)$$

Since we consider a time periodic source term with frequency  $\omega$ , the solution of (8) and the solution of (9), (10) are related by:

$$\begin{aligned} \vec{E}(t) &= \hat{E} e^{i\omega t}, \\ \vec{H}(t) &= \hat{H} e^{i\omega t}. \end{aligned}$$

The finite difference time domain method (FDTD) discretizes Maxwell's equations in space and time. The spatial domain is discretized on a uniform staggered grid with meshsizes  $h = (h_x, h_y, h_z)$ . Then, Maxwell's equations is approximated by the finite difference equations

$$\frac{\vec{E}_h^{n+1} - \vec{E}_h^n}{\tau} = \frac{1}{\epsilon} \nabla_h \times \vec{H}_h^{n+1/2} - \frac{\sigma}{\epsilon} \vec{E}_h^{n+1} + S_E e^{i\omega n\tau}, \quad (11)$$

$$\frac{\vec{H}_h^{n+1/2} - \vec{H}_h^{n-1/2}}{\tau} = -\frac{1}{\mu} \nabla_h \times \vec{E}_h^n - \frac{\sigma^*}{\mu} \vec{H}_h^{n+1/2} + S_H e^{i\omega n\tau}, \quad (12)$$

where  $\tau$  is the discrete time step,  $\vec{E}_h^n$  and  $\vec{H}_h^{n+1/2}$  are electric and magnetic field vectors approximated at time points  $n\tau$  and  $(n+1/2)\tau$  for  $n = 0, 1, \dots$ . Furthermore,  $S_H$  and  $S_E$  are discrete source terms obtained by the boundary conditions.

Now, let us assume for the discretized equations (11) and (12), that there exist initial start vectors  $\vec{E}_h^0$  and  $\vec{H}_h^0$  such that  $\vec{E}_h^n$  and  $\vec{H}_h^n$  are periodic solutions in the following sense

$$\begin{aligned} \vec{E}_h^n &= \hat{E}_h e^{i\omega n\tau}, \\ \vec{H}_h^{n+1/2} &= \hat{H}_h e^{i\omega(n+1/2)\tau}. \end{aligned}$$

Then,  $\hat{E}_h$  and  $\hat{H}_h$  satisfy the equations

$$\frac{e^{i\omega\tau} - 1}{\tau} \hat{E}_h = \frac{1}{\epsilon} \nabla_h \times \hat{H}_h e^{i\omega\tau/2} - \frac{\sigma}{\epsilon} e^{i\omega\tau} \hat{E}_h + S_E, \quad (13)$$

$$\frac{e^{i\omega\tau/2} - e^{-i\omega\tau/2}}{\tau} \hat{H}_h = -\frac{1}{\mu} \nabla_h \times \hat{E}_h - \frac{\sigma^*}{\mu} \hat{H}_h e^{i\omega\tau/2} + S_H. \quad (14)$$

This is a finite difference frequency domain (FDFD) discretization of (8).

Now, let  $\tau$  tend to zero in this system of equations. Then, considering that  $\lim_{\tau \rightarrow 0} \frac{e^{i\omega\tau} - 1}{\tau} = i\omega$ , we obtain  $\hat{E}_{h,\tau=0} = \lim_{\tau \rightarrow 0} \hat{E}_h(\tau)$  and  $\hat{H}_{h,\tau=0} = \lim_{\tau \rightarrow 0} \hat{H}_h(\tau)$  are the solution of

$$i\omega \hat{E}_{h,\tau=0} = \frac{1}{\epsilon} \nabla_h \times \hat{H}_{h,\tau=0} - \frac{\sigma}{\epsilon} \hat{E}_{h,\tau=0} + S, \quad (15)$$

$$i\omega \hat{H}_{h,\tau=0} = -\frac{1}{\mu} \nabla_h \times \hat{E}_{h,\tau=0} - \frac{\sigma^*}{\mu} \hat{H}_{h,\tau=0}. \quad (16)$$

This implies that the finite difference solution  $\hat{E}_h, \hat{H}_h$  is an approximation of  $\hat{E}, \hat{H}$  for positive and negative permittivity.

The difficulty is to find an iterative solver that calculates  $\hat{E}_h$  and  $\hat{H}_h$ . In case of  $\epsilon > 0$ , the finite difference time domain iteration method (11), (12) can be applied as an iterative solver by adding time periodic factor (using the transformation):

$$\begin{aligned} \vec{E}_h^n e^{-i\omega n\tau} &=: \hat{E}_h^n, \\ \vec{H}_h^{n+1/2} e^{-i\omega(n+1/2)\tau} &=: \hat{H}_h^n. \end{aligned}$$

This leads to the iteration algorithm

$$\begin{aligned} & \frac{e^{i\omega\tau} \hat{E}_h^{n+1} - \hat{E}_h^n}{\tau} \\ &= \frac{1}{\epsilon} \nabla_h \times \hat{H}_h^{n+1/2} e^{i\omega\tau/2} - \frac{\sigma}{\epsilon} e^{i\omega\tau} \hat{E}_h^{n+1} + S_E, \end{aligned} \quad (17)$$

$$\begin{aligned} & \frac{e^{i\omega\tau/2} \hat{H}_h^{n+1/2} - e^{-i\omega\tau/2} \hat{H}_h^{n-1/2}}{\tau} \\ &= -\frac{1}{\mu} \nabla_h \times \hat{E}_h^n - \frac{\sigma^*}{\mu} \hat{H}_h^{n+1/2} e^{i\omega\tau/2} + S_H. \end{aligned} \quad (18)$$

The explicit version of this iteration algorithm is:

$$\hat{E}_h^{n+1} = \left( \frac{\tau}{\epsilon} \nabla_h \times \hat{H}_h^{n+1/2} e^{i\omega\tau/2} + \tau S_E + \hat{E}_h^n \right) / \left( 1 + \frac{\tau\sigma}{\epsilon} \right) e^{-i\omega\tau}, \quad (19)$$

$$\hat{H}_h^{n+1/2} = \left( -\frac{\tau}{\mu} \nabla_h \times \hat{E}_h + \tau S_H + e^{-i\omega\tau/2} \hat{H}_h^{n-1/2} \right) / \left( 1 + \frac{\tau\sigma^*}{\mu} \right) e^{-i\omega\tau/2}. \quad (20)$$

However, in case of  $\epsilon < 0$ , this iteration method does not converge.

### 3.8 Stable Iteration Method for Negative Permittivity

Our aim is to modify the time iteration scheme (19) and (20) to obtain a convergent iterative solver independent of the sign of  $\epsilon$ . To this end, we keep (19) and (20) at all grid points with positive  $\epsilon > 0$  permittivity. However, we modify the discretization (13) and (14) and the iterative solver at all grid points with negative permittivity  $\epsilon < 0$ . To obtain convergence, we only have to modify equation (17) as follows:

$$\frac{e^{i\omega\tau} \hat{E}_h^n - \hat{E}_h^{n+1}}{\tau} = \frac{1}{\epsilon} \nabla_h \times \hat{H}_h^{n+1/2} e^{i\omega\tau/2} - \frac{\sigma}{\epsilon} \hat{E}_h^{n+1} + S_E.$$

The explicit version of this iteration algorithm is:

$$\hat{E}_h^{n+1} = \frac{1}{1 - \frac{\tau\sigma}{\epsilon}} \left( -\frac{\tau}{\epsilon} \nabla_h \times \hat{H}_h^{n+1/2} e^{i\omega\tau/2} - \tau S_E - \hat{E}_h^n e^{i\omega\tau} \right)$$

The total iterative solver can be written as

$$\begin{pmatrix} \hat{E}_h^{n+1} \\ \hat{H}_h^{n+1/2} \end{pmatrix} = M_\tau \begin{pmatrix} \hat{E}_h^n \\ \hat{H}_h^{n-1/2} \end{pmatrix} + B_\tau.$$

Showing convergence of this iterative method independent of the sign of  $\epsilon$  and independent of the meshsize  $h$  requires a detailed analysis.

Here, let us assume that (21) converges. Then, there is a fixed point  $\hat{E}_h$  and  $\hat{H}_h$  of the iterative solver (21). Thus,  $\hat{E}_h$  and  $\hat{H}_h$  satisfy the equations

$$\begin{aligned}
\frac{e^{i\omega\tau} - 1}{\tau} \hat{E}_h &= \frac{1}{\epsilon} \nabla_h \times \hat{H}_h e^{i\omega\tau/2} \\
&\quad - \frac{\sigma}{\epsilon} \left(1 - \frac{(1 - e^{i\omega\tau})(1 + \text{sign}(\epsilon))}{2}\right) \hat{E}_h + S_E, \\
\frac{e^{i\omega\tau/2} - e^{-i\omega\tau/2}}{\tau} \hat{H}_h &= -\frac{1}{\mu} \nabla_h \times \hat{E}_h \\
&\quad - \frac{\sigma^*}{\mu} \hat{H}_h e^{i\omega\tau/2} + S_H.
\end{aligned}$$

This shows that the finite difference solution  $\hat{E}_h, \hat{H}_h$  is an approximation of  $\hat{E}, \hat{H}$ .

## 4 Beam Propagation

### 4.1 Paraxial Approximation

The paraxial approximation is an approximation of the scalar Helmholtz equation.

$$(\Delta + k^2)E(x, y, z) = 0.$$

Let  $k_0$  be an average value of  $k$ . Inserting the ansatz

$$E = e^{-ik_0 z} \Psi(x, y, z)$$

in the scalar Helmholtz equation leads to

$$-\Delta \Psi + 2ik_0 \frac{\partial \Psi}{\partial z} + (k_0^2 - k^2) \Psi = 0.$$

In the paraxial approximation, we neglect the term  $\frac{\partial^2 \Psi}{\partial z^2}$ . This leads to:

$$-\frac{\partial^2 \Psi}{\partial x^2} - \frac{\partial^2 \Psi}{\partial y^2} + 2ik_0 \frac{\partial \Psi}{\partial z} + (k_0^2 - k^2) \Psi = 0.$$

In the case that  $k = k_0$  is constant, we obtain

$$-\frac{\partial^2 \Psi}{\partial x^2} - \frac{\partial^2 \Psi}{\partial y^2} + 2ik \frac{\partial \Psi}{\partial z} = 0.$$

## 4.2 Beam Propagation Method BPM

Let us write the paraxial approximation as follows:

$$2ik_0 \frac{\partial \Psi}{\partial z} = \frac{\partial^2 \Psi}{\partial x^2} + \frac{\partial^2 \Psi}{\partial y^2} - (k_0^2 - k^2) \Psi.$$

Let  $\Omega = \mathcal{D} \times ]0, L[$ , then one can apply

- FE or FD in  $x, y$ -direction
- Crank-Nicolson in  $z$ -direction.

Let  $\Psi^l(x, y)$  be the approximation of  $\Psi(x, y, \tau l)$ , where  $\tau$  is the time step. Then,  $\Psi^l(x, y)$  is defined by the equations:

$$2ik_0 \frac{\Psi^{l+1} - \Psi^l}{\tau} = \frac{1}{2} \left( \frac{\partial^2 \Psi^{l+1}}{\partial x^2} + \frac{\partial^2 \Psi^{l+1}}{\partial y^2} - (k_0^2 - k^2) \Psi^{l+1} + \frac{\partial^2 \Psi^l}{\partial x^2} + \frac{\partial^2 \Psi^l}{\partial y^2} - (k_0^2 - k^2) \Psi^l \right)$$

$$\Psi^0(x, y) = \Psi^{\text{initial}}(x, y) \quad (\text{initial condition})$$

- Additional boundary conditions are needed.
- Lenses and mirrors can be discretized by a phase shift.

$$\Psi^{l+1} = \left( E - \frac{\tau}{2ik_0} \frac{1}{2} \left( \frac{\partial^2}{\partial x^2} + \frac{\partial^2}{\partial y^2} + (k_0^2 - k^2) \cdot + \right) \right)^{-1} \left( \Psi^l + \frac{\tau}{2ik_0} \frac{1}{2} \left( \frac{\partial^2 \Psi^l}{\partial x^2} + \frac{\partial^2 \Psi^l}{\partial y^2} + (k_0^2 - k^2) \Psi^l \right) \right).$$

## 5 Basic Properties of a Laser

### 5.1 Elements of a Laser

A laser consists mainly of the following three elements (see Figure 6) :

1. Laser medium: collection of atoms, molecules, ions or a semiconductor crystal:
  - gas laser
  - solid state lasers
  - semiconductor lasers
  - fiber laser
2. Pumping process to excite the atoms (molecules) into higher quantum mechanical energy levels.
3. Suitable optical feedback elements
  - as a laser amplifier (one pass of the beam)
  - as a laser oscillator (bounce back and forth of the laser beam)

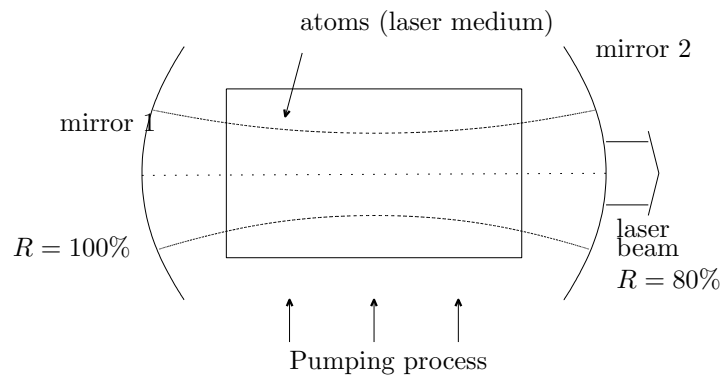


Figure 6: Basic Properties of a Laser

1. Population inversion (see Figure 7)
2. Amplification of light (electromagnetic radiation) within a certain narrow band of frequencies. The amplification depends on the population inversion.
3. Oscillation: There must be more gain than loss of the beam. Reasons of loss are:

- loss by medium
  - not accurate construction of the mirrors
  - output
4. Eigenmodes of a laser (e.g. Gauss modes , see Figure 8 ).
- deformation of the crystal
  - gain, lenses
  - different refraction index

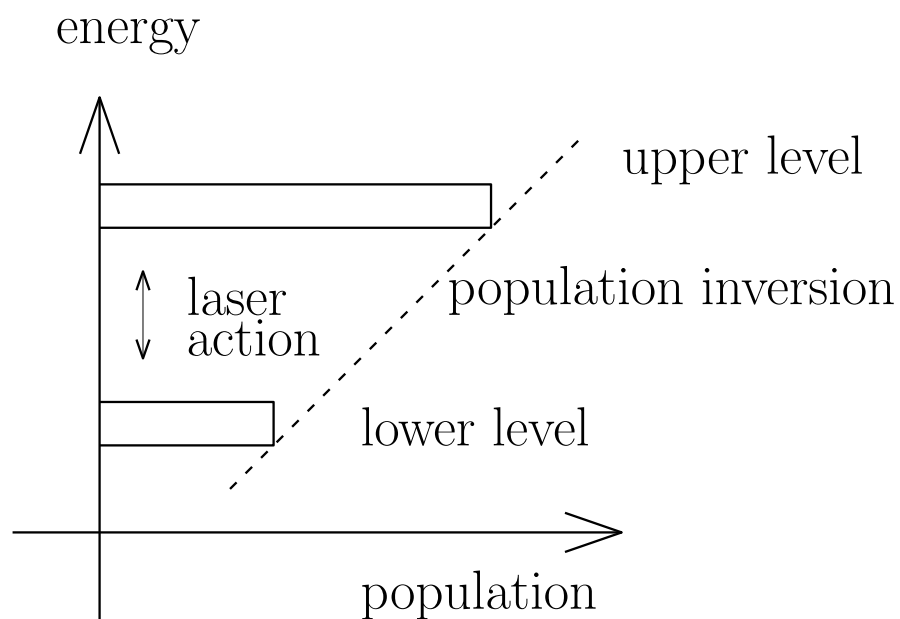


Figure 7: Population inversion

## 5.2 Atomic Energy Levels, Spontaneous Emission and Stimulated Transition

Light of a certain wavelength is emitted if a transition between two energy levels  $E_2 \rightarrow E_1$  takes place  
 “ jump of electrons “ .



[0, 0] Gaussian

[0, 1] Gaussian

[1, 1] Gaussian

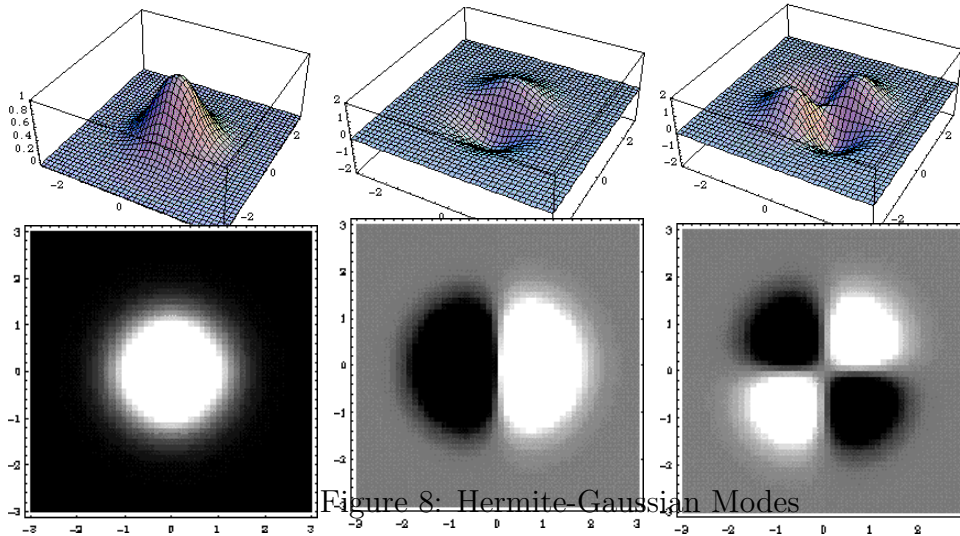


Figure 8: Hermite-Gaussian Modes

**Formula 2.** The frequency of the emitted light is

$$\omega_{21} = \frac{E_2 - E_1}{\hbar}, \quad (21)$$

where

$$\hbar = \frac{h}{2\pi}, \quad h = 6.626 \cdot 10^{-34} \text{ Js} \quad \text{Planck's constant.}$$

Notation for wavelength:  $1\mu\text{m} = 10000 \text{ \AA}$

Due to this formula, the energy levels can be described by

- $\frac{1}{\lambda}$  in  $\text{cm}^{-1}$  where  $\lambda$  is the wavelength of the corresponding wave and
- by a value with unit  $\text{eV}$ .

Transition from  $E_2 \rightarrow E_1$  takes place only with a little additional energy:

- spontaneous emission: energy from small movements of the atoms
- stimulated emission: energy from absorption

Let  $N_i$  be the number of atoms with energy level  $E_i$ .

Within a short period of time a certain percentage of atoms make a transition to a lower level.

This can be described by the following ODE:

$$\left. \frac{dN_2}{dt} \right|_{\text{spont}} = -\gamma N_2 = -\frac{N_2}{\tau},$$

where

- $\gamma$  is called energy-decay rate and
- $\tau = \frac{1}{\gamma}$  is called lifetime.

The solution of this ODE is:

$$N_2(t) = N_2(0)e^{-\frac{t}{\tau}}$$

If an external radiation signal is applied to the atom, then stimulated transitions occur: “atom reacts like an antenna”.

Let  $n(t)$  be the photon density of the radiation.

Then, there is a constant  $K$  such that (see Figure) 9

$$\begin{aligned} \left. \frac{dN_2}{dt} \right|_{\text{stim.upward}} &= Kn(t)N_1(t), \quad (\text{absorption}) \\ \left. \frac{dN_2}{dt} \right|_{\text{stim.downward}} &= -Kn(t)N_2(t) \quad (\text{stimulated emission}). \end{aligned}$$

This implies:

$$\left. \frac{dN_2}{dt} \right|_{\text{total}} = Kn(t)(N_1(t) - N_2(t)) - \gamma_{21}N_2(t) = -\left. \frac{dN_1}{dt} \right|_{\text{total}}.$$

The total rate of signal stimulated transition between two energy levels is:

$$Kn(t) \cdot (N_1(t) - N_2(t)).$$

The energy transfer of stimulated transition by a signal is

$$\frac{dU_a}{dt} = Kn(t)(N_1(t) - N_2(t)) \cdot \hbar\omega,$$

where  $U_a$  is the energy density.

The energy transfer changes the photon density of the signal by:

$$\frac{dn(t)}{dt} = -K(N_1(t) - N_2(t)) \cdot n(t). \quad (22)$$

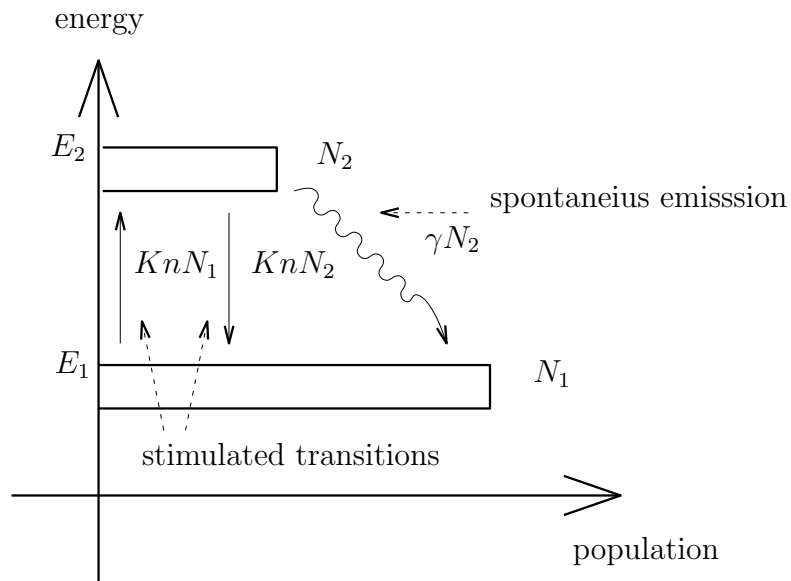


Figure 9: Stimulated transition

- Absorption (attenuation):  $N_1(t) > N_2(t)$
- Population inversion:  $N_1(t) < N_2(t)$   
 → net amplification of a signal

### 5.3 Pumping Process and Population Inversion

Population inversion means that

$$N_1 < N_2$$

where  $N_i$  is the number of atoms with energy level  $E_i$ , such that  $E_2 > E_1$ . In equilibrium there is no population inversion. The reason for this is Boltzmann's Principle of equilibrium:

**Theorem 2** (Boltzmann's Principle). *In case of equilibrium the populations  $N_1$  and  $N_2$  depend on the temperature:*

$$\frac{N_2}{N_1} = \exp\left(-\frac{E_2 - E_1}{kT}\right).$$

*This implies*

$$N_1 - N_2 = N_1 \left(1 - e^{-\frac{E_2 - E_1}{kT}}\right).$$

To obtain population inversion, a pumping process is needed, which destroys the state of equilibrium. Figure 10 shows a model of three level pumping process.

Let

- $R_{p0}$  be the pumping rate (atoms/sec),
- $\eta_p$  the pumping efficiency such that  $R_p = \eta_p R_{p0}$  and
- $\gamma_{ij}$  the decay rate from level  $E_i$  to  $E_j$ .

The following formulas describe the pumping process (without stimulated transitions):

$$\begin{aligned}\frac{dN_2}{dt} &= R_p - \gamma_{21}N_2 \\ \frac{dN_1}{dt} &= \gamma_{21}N_2 - \gamma_{10}N_1\end{aligned}$$

If  $\frac{dN_i}{dt} = 0$ , then we get

$$N_2 > N_1 \text{ (population inversion)} \Leftrightarrow \tau_{10} < \tau_{21}$$

## 5.4 Example of Scalar Rate Equations

Let us consider a four level pumping process according [8].

Let us abbreviate

$$N = N_2 - \frac{g_2 N_1}{g_1}$$

then, the scalar rate equations are

$$\frac{\partial N}{\partial t} = -\gamma N n \sigma c - \frac{N + N_{tot}(\gamma - 1)}{\tau_f} + R_p(N_{tot} - N) \quad (23)$$

$$\frac{\partial n}{\partial t} = N n \sigma c - \frac{n}{\tau_c} + S. \quad (24)$$

The unknowns of these equations are

- $N$ : population inversion  $N = N_2 - \frac{g_2 N_1}{g_1}$ .

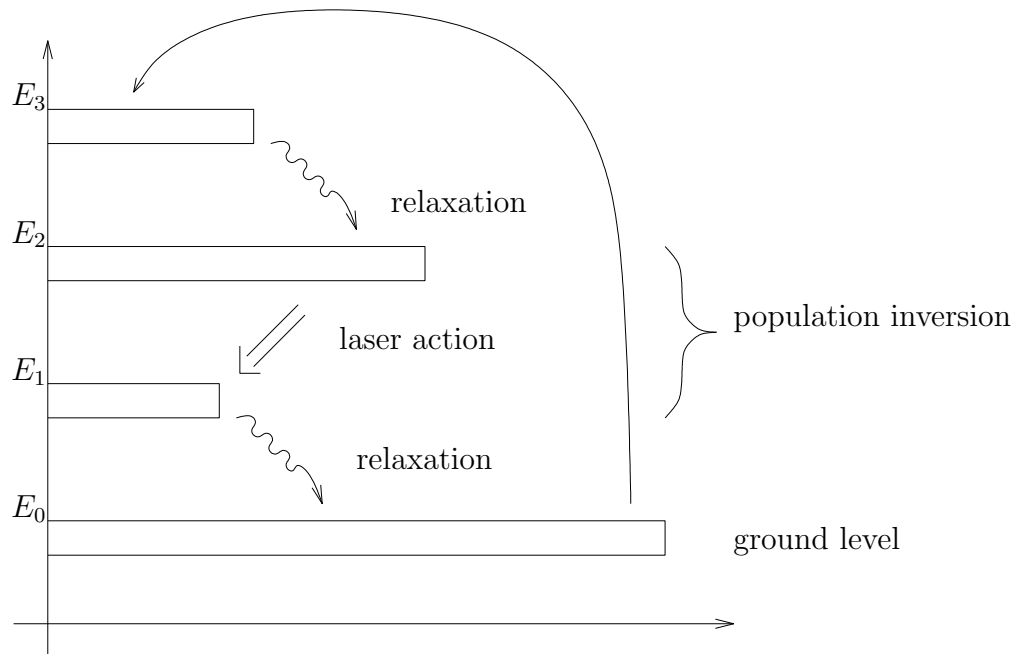


Figure 10: Three-level laser pumping process

- $n$ : photon density

Parameters for Ruby are (see [8] section 2.2):

- $g_1, g_2$ : degeneracy factors for quantum energy levels of Ruby:
  - $g(N_1) = 4$
  - $g(N_2(R_1)) = 2$ , where  $R_1$  is the green band with wavelength  $6943 \text{ \AA}$
  - $g(N_2(R_2)) = 2$ , where  $R_2$  is the blue band with wavelength  $6929 \text{ \AA}$
- $\sigma$ : stimulated emission cross section  $\sigma_{21} = 2.5 \cdot 10^{-20} \text{ cm}^2$
- $N_{tot}$ :  $1.58 \cdot 10^{19} \text{ ions/cm}^3$  is the maximal population inversion.
- $R_{p0}$ : pumping rate *atoms/sec*
- $\eta_p$ : Quantum efficiency 0.7
- $\tau_f$ :  $3 \text{ ms}$  (see page 15 in [8]) for  $R_1$  line.

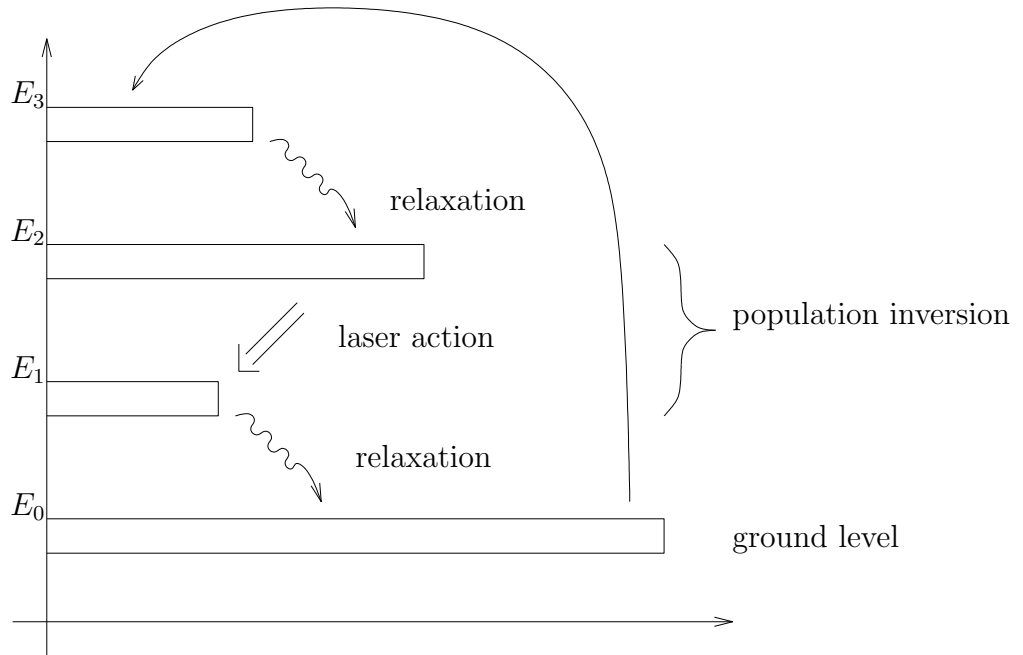


Figure 11: Four-level laser pumping process

- $S$  is a small value needed for the start up of a laser.
- $\tau_c$ : decay rate of photons.

## 5.5 Laser Amplification and Oscillation Condition

Let us assume that the optical wave can be modeled by

$$\begin{aligned}\tilde{E}(z, t) &= \exp(j\omega t)E(z) \\ E(z) &= \exp(-jkz + \alpha_m z) = \exp(-jkz)u(z) \\ u(z) &= \exp(\alpha_m z).\end{aligned}$$

This implies that

$$\tilde{E}(z, t) = \exp(j\omega t) \cdot \exp(-jkz + \alpha_m z)$$

Thus, a constant phase shift is obtained at  $\omega t = kz$ .

Since  $t = z/c$  in vacuum, we get

$$k = \frac{\omega}{c}.$$

(By  $k^2 = \mu\epsilon\omega^2$  in Section 2.3, we obtain  $c = \frac{1}{\sqrt{\mu\epsilon}}$  in vacuum.)

Now, let us model the optical wave by

$$\begin{aligned}\tilde{E}(z, t) &= \exp(j\omega t)E(z) \\ E(z) &= \exp(-j\omega z/c + \alpha_m z) = \exp(-j\omega z/c)u(z) \\ u(z) &= \exp(\alpha_m z).\end{aligned}$$

An increase of the photons leads to a gain of the optical wave:

$$|E(z)|^2 = |E_0|^2 \exp(+2\alpha_m z)$$

for the intensity of the optical wave, which is proportional to the photon density. Let  $r_i$  be the reflection coefficient at the mirrors  $M_i, i = 1, 2$ .

Let  $L_m$  be the length of the amplification medium.

Let  $L$  be the length of the laser medium.

Figure 12 shows one round trip of the optical wave.

Then, the minimal amplification by one round trip is:

$$\exp(4\alpha_m L_m)$$

and the round trip phase shift is:

$$\exp(-2j\omega L/c)$$

Then, we get

$$r_1 r_2 \exp(2\alpha_m L_m - j2\omega L/c) = 1.$$

This implies

$$\alpha_m = \frac{1}{2L_m} \ln \left( \left| \frac{1}{r_1} \right| \cdot \left| \frac{1}{r_2} \right| \right)$$

The energy density of the electrical field is (see [3]):

$$\frac{\epsilon}{2}|E|^2$$

Thus, by (21), we obtain

$$n(z) = \frac{\epsilon}{2\hbar\omega}|E|^2 = \frac{\epsilon}{2\hbar\omega}|E_0|^2 \exp(+2\alpha_m z)$$

Since  $z = ct$ , we obtain

$$n(t) = \frac{\epsilon}{2\hbar\omega}|E|^2 = \frac{\epsilon}{2\hbar\omega}|E_0|^2 \exp(+2\alpha_m ct).$$

By (22), we get

$$K(N_2 - N_1) = 2\alpha_m c \quad (25)$$

Consequences:

$$2\omega L/c \in 2\pi\mathbb{Z} \Rightarrow \text{only certain frequencies!}$$

$$|r_1 r_2| \exp(2\alpha_m L_m) = 1 \Rightarrow N_2 - N_1 \geq \frac{c}{K} \frac{1}{2L_M} \ln \left( \left| \frac{1}{r_1} \right| \cdot \left| \frac{1}{r_2} \right| \right)$$

This is the threshold inversion population (density).

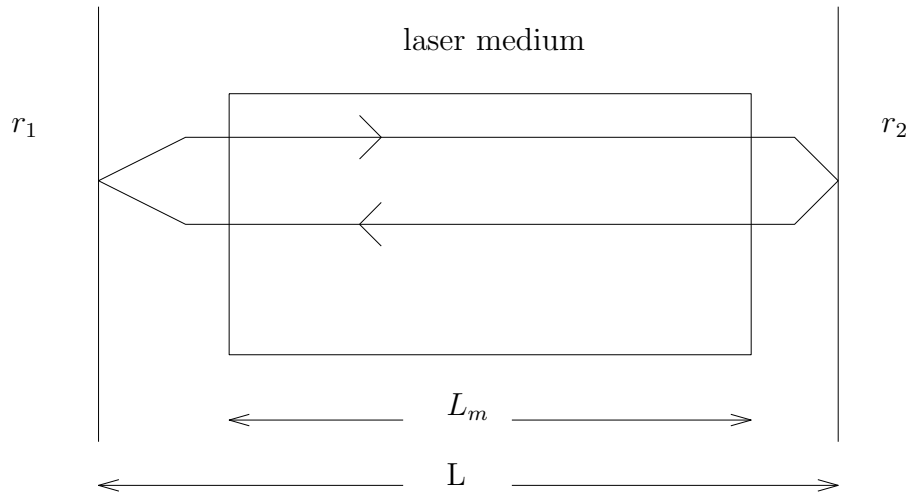


Figure 12: Round trip in laser resonator

## 6 Numerical Discretization of a Scalar Rate Equation

Consider the equations (23) and (24) according section 5.4

$$\begin{aligned} \frac{\partial N}{\partial t} &= -\gamma N n \sigma c - \frac{N + N_{tot}(\gamma - 1)}{\tau_f} + R_p(N_{tot} - N) \\ \frac{\partial n}{\partial t} &= N n \sigma c - \frac{n}{\tau_c} + S \end{aligned}$$



The initial values are

$$N(0) = N_0 \quad \text{and} \quad n(0) = n_0.$$

To discretize the unknowns

- $N$ : population inversion  $N = N_2 - N_1$ .
- $n$ : photon density

let us use an explicit / implicit Euler discretization with meshsize  $\tau$ .

Let

- $N_s$  be the approximation of  $N(\tau s)$  and
- $n_s$  be the approximation of  $n(\tau s)$ .

We need a discretization which guarantees that

$$n_s > 0 \quad \text{and} \quad N_s > 0$$

independent of  $s \in \mathbb{N}$ . Let us assume that  $n_s > 0$  and  $N_s > 0$  for a fixed  $s$ .

- Formula for  $N_{s+1}$ : The factor  $1/\tau + \gamma * n_s * \sigma * c + 1/\tau_f + R_p$  is positive. Therefore we apply a pure implicit method:

$$N_{s+1} = (N_s/\tau - N_{tot} * (\gamma - 1) / \tau_f + R_p * N_{tot}) / (1/\tau + \gamma * n_s * \sigma * c + 1/\tau_f + R_p);$$

- Formula for  $n_{s+1}$ :

– If  $c\sigma N_s - 1/\tau_c > 0$ , then we apply an explicit method:

$$n_{s+1} = n_s + \tau * (n_s(c\sigma N_s - 1/\tau_c) + S)$$

– If  $c\sigma N_s - 1/\tau_c \leq 0$ , then we apply an implicit method:

$$n_{s+1} = (n_s/\tau + S) / (1/\tau - c\sigma N_s + 1/\tau_c)$$

This discretization guarantees that  $n_{s+1} > 0$  and  $N_{s+1} > 0$ . By induction we get  $n_s > 0$  and  $N_s > 0$  for every  $s \in \mathbb{N}$ .

Figure 13 depicts a numerical result.

The peak of the photon density after switching on the laser resonator leads to the construction of pulsed lasers.

Output power of  $n(t)$ .

$N(t)$  population inversion

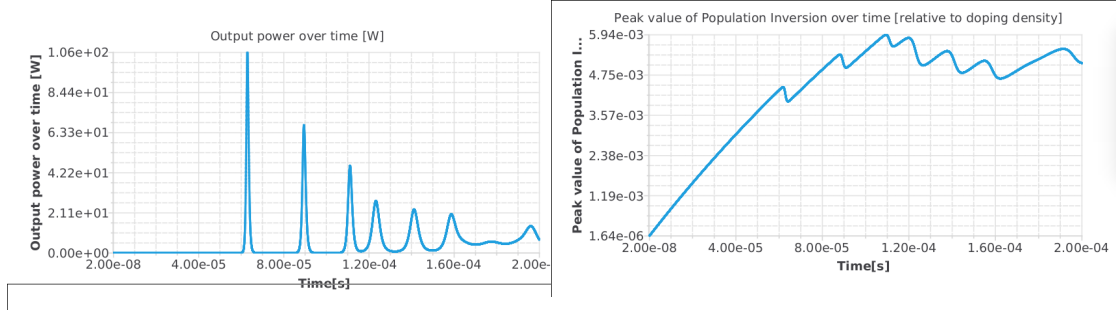


Figure 13: Numerical result

## 7 Mode-Analysis

### 7.1 Gauss Mode Analysis

#### 7.1.1 The Lowest Order Gauss-Mode

The paraxial approximation leads to:

$$-\frac{\partial^2 \Psi}{\partial x^2} - \frac{\partial^2 \Psi}{\partial y^2} + 2ik \frac{\partial \Psi}{\partial z} = 0.$$

To solve the paraxial approximation, let us make the ansatz

$$\Psi(x, y, z) = A(z) \exp\left(-ik \frac{x^2 + y^2}{2q(z)}\right),$$

where  $A(z)$  and  $q(z)$  are unknown functions.

This leads to:

$$\begin{aligned} \frac{\partial \Psi}{\partial x} &= A(z) \exp\left(-ik \frac{x^2 + y^2}{2q(z)}\right) \left(-ik \frac{2x}{2q(z)}\right) \\ \frac{\partial^2 \Psi}{\partial x^2} &= A(z) \exp\left(-ik \frac{x^2 + y^2}{2q(z)}\right) \left(-k^2 \frac{x^2}{q^2(z)}\right) \\ &\quad + A(z) \exp\left(-ik \frac{x^2 + y^2}{2q(z)}\right) \left(-ik \frac{1}{q(z)}\right) \\ \frac{\partial \Psi}{\partial z} &= A'(z) \exp\left(-ik \frac{x^2 + y^2}{2q(z)}\right) \end{aligned}$$

$$+A(z) \exp\left(-ik\frac{x^2+y^2}{2q(z)}\right) (-ik(x^2+y^2))(-1)\frac{1}{2q^2}q'.$$

Thus, we get

$$\begin{aligned} 0 &= -\frac{\partial^2\Psi}{\partial x^2} - \frac{\partial^2\Psi}{\partial y^2} + 2ik\frac{\partial\Psi}{\partial z} \\ &= A(z) \exp\left(-ik\frac{x^2+y^2}{2q(z)}\right) \\ &\quad \cdot \left(k^2\frac{1}{q^2}(x^2+y^2) - k^2\frac{1}{q^2}q'(x^2+y^2) + 2ik\frac{1}{q} + 2ik\frac{A'}{A}\right) \\ 0 &= \frac{k^2}{q^2}(x^2+y^2)(1-q') + 2ik\left(\frac{1}{q} + \frac{A'}{A}\right). \end{aligned}$$

This equation leads to the ODE's

$$\frac{\partial q}{\partial z} = 1 \quad \text{and} \quad \frac{\partial A}{\partial z} = -A \cdot \frac{1}{q}.$$

The unique solutions of these equations are

- $q(z) = q_0 + z$ , where  $q_0$  and  $z_0$  are constants.
- $A(z) = A_0\frac{q_0}{q(z)}$ .

Thus, lowest order Gauss mode is

$$\begin{aligned} E(x, y, z) &= e^{-ikz}\Psi(x, y, z) \\ &= A_0\frac{q_0}{q_0+z} \exp\left(ik\left(-z - \frac{x^2+y^2}{2(q_0+z)}\right)\right) \end{aligned}$$

Let us normalize the amplitude of this mode by  $q_0A_0 = 1$ . Then,

$$E(x, y, z) = \frac{1}{q_0+z} \exp\left(-ik\left(z + \frac{x^2+y^2}{2(q_0+z)}\right)\right)$$

Now, let us study the spot size, beam waist and the energy of the lowest order Gauss mode.

**Definition 3.** *The spot size is defined by the radius  $r$  such that*

$$e^{-1} = \frac{|E(z, r)|}{|E(z, 0)|}$$

Write

$$\frac{1}{q_0 + z} = \frac{1}{q(z)} = \frac{1}{R(z)} - i \frac{\lambda}{\pi w(z)}$$

where  $R(z)$  and  $w(z)$  are real valued functions. This means

$$\frac{1}{q_0 + z} = (\operatorname{Re}(q_0) + z) \frac{1}{\operatorname{Im}(q_0)^2 + (\operatorname{Re}(q_0) + z)^2} - i \frac{\operatorname{Im}(q_0)}{\operatorname{Im}(q_0)^2 + (\operatorname{Re}(q_0) + z)^2}$$

and

$$\begin{aligned} \frac{1}{R(z)} &= (\operatorname{Re}(q_0) + z) \frac{1}{\operatorname{Im}(q_0)^2 + (\operatorname{Re}(q_0) + z)^2} \\ R(z) &= \frac{\operatorname{Im}(q_0)^2 + (\operatorname{Re}(q_0) + z)^2}{\operatorname{Re}(q_0) + z} \\ &= (\operatorname{Re}(q_0) + z) \left( 1 + \frac{\operatorname{Im}(q_0)^2}{(\operatorname{Re}(q_0) + z)^2} \right)^2 \end{aligned} \quad (26)$$

$$\begin{aligned} w(z) &= \frac{\lambda \operatorname{Im}(q_0)^2 + (\operatorname{Re}(q_0) + z)^2}{\pi \operatorname{Im}(q_0)} \\ &= \frac{\lambda}{\pi} \left( \operatorname{Im}(q_0) + \frac{(\operatorname{Re}(q_0) + z)^2}{\operatorname{Im}(q_0)} \right) \end{aligned} \quad (27)$$

$$(28)$$

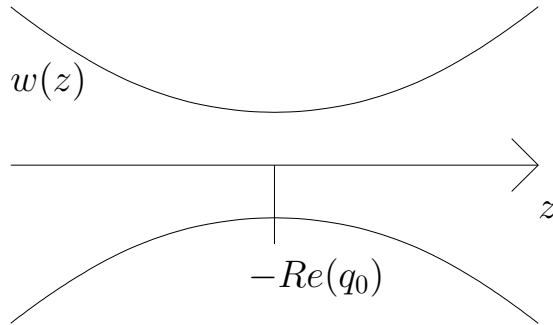


Figure 14: Beam waist of a Gaussian beam.

Phase shift:  $\exp\left(-ik\left(z + \frac{x^2+y^2}{2R(z)}\right)\right)$

By this analysis of the Gaussian beam, we get:

- Phase shift: The phase shift of the beam  $E(x, y, z)$  behaves like

$$\exp\left(-ik\left(z + \frac{x^2 + y^2}{2R(z)}\right)\right)$$

- Spot size: The spot size is  $w(z)$ .
- Figure 14 shows the beam waist  $w(z)$ .

Now, let us analyze the energy of the beam at every slice  $z = \text{constant}$ . To this end, observe that

$$|q_0 + z|^2 = \frac{\pi |\text{Im}(q_0)|}{\lambda} |w(z)|$$

$$\begin{aligned} \int_{\mathbb{R}^2} |\exp(-b(x^2 + y^2))|^2 d(xy) &= \int_0^\infty \int_0^{2\pi} \exp(-2br^2) r \, d\varphi dr \\ &= 2\pi \frac{1}{-4b} \exp(-2br^2) \Big|_0^\infty \\ &= \frac{\pi}{2b} \end{aligned}$$

$$\begin{aligned} \int_{\mathbb{R}^2} |E|^2 d(xy) &= \left| \frac{A_0 q_0}{q_0 + z} \right|^2 \int_{\mathbb{R}^2} \left| \exp\left(-ik\left(\frac{x^2 + y^2}{2(q_0 + z)}\right)\right) \right|^2 \\ &= \left| \frac{A_0 q_0}{q_0 + z} \right|^2 \int_{\mathbb{R}^2} \left| \exp\left(-\frac{\lambda k}{\pi} \frac{(x^2 + y^2)}{w(z)}\right) \right|^2 \\ &= \left| \frac{A_0 q_0}{q_0 + z} \right|^2 \frac{\pi}{2} \frac{\pi}{\lambda k} |w(z)| \\ &= \frac{|A_0 q_0|^2}{\frac{\lambda |\text{Im}(q_0)|}{\pi} |w(z)|} \frac{\pi}{2} \frac{\pi}{\lambda k} |w(z)| \\ &= \frac{|A_0 q_0|^2}{|\text{Im}(q_0)|} \frac{\pi}{2} \frac{\pi^2}{\lambda^2 k} \end{aligned}$$

This shows that the energy

$$\int_{\mathbb{R}^2} |E|^2 d(xy) = \frac{|A_0 q_0|^2}{|\text{Im}(q_0)|} \frac{\pi}{2} \frac{\pi^2}{\lambda^2 k}$$

is independent of  $z$ .

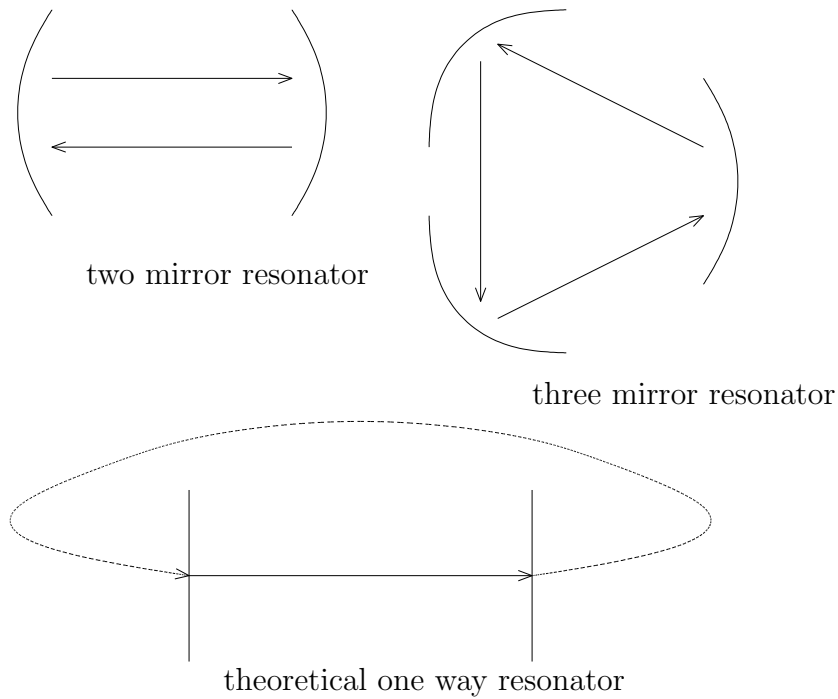


Figure 15: Types of resonators.

### 7.1.2 Gauss Mode in an Aperture

There exists several types of resonators (see Figure 16). Here, let us study a one way resonator. Other resonators can be transformed to a one way resonator.

This means that a beam travels from left to right and that the beam at the right points  $z = L$  travels directly to the first point  $z = 0$ .

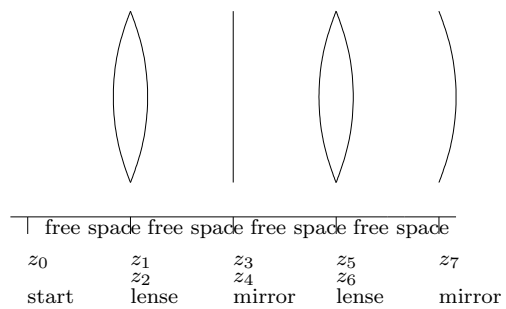
Let  $\Omega = \Omega_2 \times [0, L]$  be a resonator geometry.

Let us assume that there are  $n$  apertures in the resonator.

The start points of these apertures are

$$0 = z_0 \leq z_1 \leq z_2 \leq \dots \leq z_n = L.$$

Let us shift the origin of the Gauss-modes in the resonator to these points



such that

$$E_i(x, y, z) = \mathcal{A}_i \frac{1}{q_i + (z - z_i)} \exp \left( -ik \left( (z - z_i) + \frac{x^2 + y^2}{2(q_i + (z - z_i))} \right) \right)$$

where  $\mathcal{A}_i := A_i q_i$ .

Then,  $E_i(x, y, z)$  is the approximation of the electrical field in the subdomain

$$\begin{aligned} \Omega_2 \times ]z_{i-1}, z_i[ & \text{ if } z_{i-1} \neq z_i \\ \Omega_2 \times [z_{i-1}, z_i] & \text{ if } z_{i-1} = z_i \end{aligned}$$

The change of the Gauss-mode is described by ABCD matrices

$$M_i = \begin{pmatrix} A^i & B^i \\ C^i & D^i \end{pmatrix}$$

Then, the beam parameter  $q_i$  changes as follows

$$q_i = \frac{A^i q_{i-1} + B^i}{C^i q_{i-1} + D^i} =: M_i[q_{i-1}].$$

**Lemma 2.**

$$M_{i+1}[M_i[q_{i-1}]] = (M_{i+1}M_i)[q_{i-1}]$$

This lemma can be proved by a direct calculation.

Another way to prove this lemma is to use that ABCD matrices describe the behavior of rays. To this end, one has to apply the mapping

$$\begin{pmatrix} r_{in} \\ r'_{in} \end{pmatrix} \mapsto q = \frac{r_{in}}{r'_{in}}.$$

Then, the above lemma follows by the formula of matrix multiplication.

### 7.1.3 Ray Optics and ABCD Matrix

Originally, ABCD matrices were used to describe the behavior of rays in optical apertures.

An optical ray can be described by

- the radius  $r(z)$  and
- the slope  $r'(z)$ .

The change of an optical ray is described by

$$\begin{pmatrix} r_{\text{out}} \\ r'_{\text{out}} \end{pmatrix} = \begin{pmatrix} A & B \\ C & D \end{pmatrix} \begin{pmatrix} r_{\text{in}} \\ r'_{\text{in}} \end{pmatrix}$$

**Example 6** (Ray-matrix of free space).

$$\begin{pmatrix} r_{\text{out}} \\ r'_{\text{out}} \end{pmatrix} = \begin{pmatrix} 1 & \frac{L}{n_0} \\ 0 & 1 \end{pmatrix} \begin{pmatrix} r_{\text{in}} \\ r'_{\text{in}} \end{pmatrix}$$

Here, observe that the refractive index is  $n_0 = \frac{c}{v}$ , where  $v$  is the velocity of the optical wave in the medium and  $c$  is the velocity in vacuum.

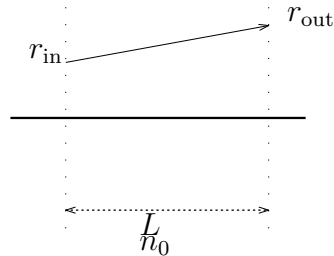


Figure 16: Ray in free space.



#### 7.1.4 ABCD Matrix of free space

By

$$E_i(x, y, z) = E_{i-1}(x, y, z)$$

we obtain

$$\begin{aligned} \mathcal{A}_i \frac{1}{q_i + (z - z_i)} \exp\left(-ik\left((z - z_i) + \frac{x^2 + y^2}{2(q_i + (z - z_i))}\right)\right) \\ = \mathcal{A}_{i-1} \frac{1}{q_{i-1} + (z - z_{i-1})} \exp\left(-ik\left((z - z_{i-1}) + \frac{x^2 + y^2}{2(q_{i-1} + (z - z_{i-1}))}\right)\right) \end{aligned}$$

↓

$$q_i + (z - z_i) = q_{i-1} + (z - z_{i-1})$$

$$\text{and } \mathcal{A}_i \exp(-ik(z - z_i)) = \mathcal{A}_{i-1} \exp(-ik(z - z_{i-1}))$$

↓

$$q_i = q_{i-1} + (z_i - z_{i-1})$$

$$\text{and } \mathcal{A}_i = \mathcal{A}_{i-1} \exp(ik(-(z_i - z_{i-1})))$$

This shows

**Formula 3** (ABCD matrix of free space).

$$\begin{pmatrix} A & B \\ C & D \end{pmatrix} = \begin{pmatrix} 1 & z_i - z_{i-1} \\ 0 & 1 \end{pmatrix}$$

and

$$\mathcal{A}_i = \mathcal{A}_{i-1} \exp(ik(-(z_i - z_{i-1})))$$

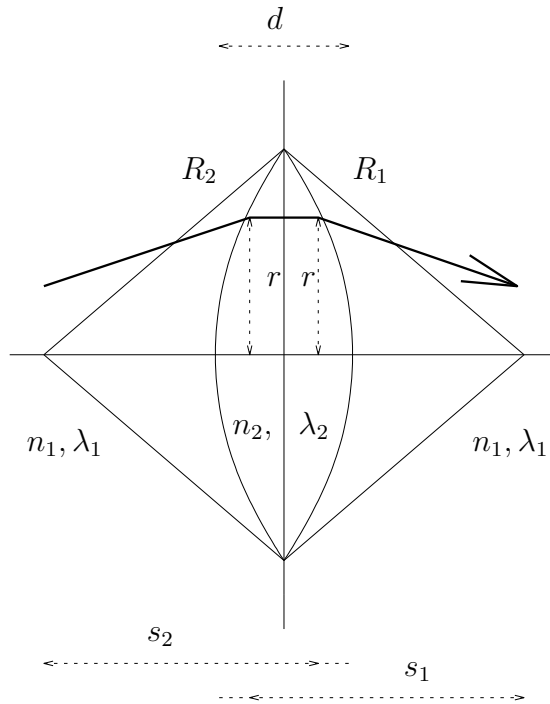


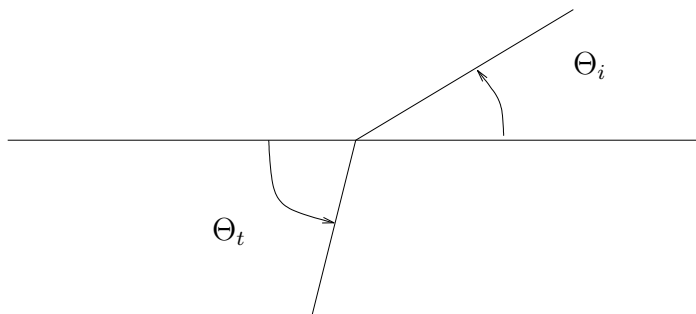
Figure 17: Phase shift of a lens.

### 7.1.5 ABCD Matrix of a lens

In ray optics the ABCD matrix of a lens is calculated by Snellius law:

$$n_i \sin \Theta_i = n_t \sin \Theta_t,$$

where the angles  $\Theta_i$  and  $\Theta_t$  are defined by the following figure:



Let us shift the lense such that  $z_{i-1} = z_i = 0$ . The lense leads to a phase shift

$$\exp(-i2\pi\varphi(r))$$

where  $r = \sqrt{x^2 + y^2}$  such that

$$E_i(x, y, z) = E_{i-1}(x, y, z) \exp(-i2\pi\varphi(\sqrt{x^2 + y^2})) \quad (29)$$

Let us first calculate this phase shift. By Figure 17, we see that

$$\begin{aligned} s_2^2 + r^2 &= R_2^2 \\ s_1^2 + r^2 &= R_1^2. \end{aligned}$$

Observe the  $R_1 + R_2 - d$  is the distance of the to focus points of the lense.

Let us compose the beam by several rays. Then, the length of the way of the ray through the media  $n_1$  is:

$$\begin{aligned} (R_1 + R_2 - d) - s_1 + (R_1 + R_2 - d) - s_2 \\ = 2(R_1 + R_2 - d) - s_1 - s_2 \end{aligned}$$

and the length of the way of the ray through the media  $n_2$  is:

$$\begin{aligned} R_1 + R_2 - d - (2(R_1 + R_2 - d) - s_1 - s_2) \\ = -(R_1 + R_2 - d) + s_1 + s_2. \end{aligned}$$

To calculate, the phase shift we have to divide by the wavelength  $\lambda_1$  and  $\lambda_2$ , respectively:

$$\begin{aligned} \frac{2(R_1 + R_2 - d) - s_1 - s_2}{\lambda_1} + \frac{-(R_1 + R_2 - d) + s_1 + s_2}{\lambda_2} \\ = Q + (s_1 + s_2) \left( \frac{1}{\lambda_2} - \frac{1}{\lambda_1} \right) \\ = Q + (s_1 + s_2) \frac{1}{\lambda_1} \left( \frac{\lambda_1}{\lambda_2} - 1 \right), \end{aligned}$$

where  $Q$  is a constant term independent of  $r$ . Thus, the principal part of the phase shift is contained in

$$(s_1 + s_2) \frac{1}{\lambda_1} \left( \frac{\lambda_1}{\lambda_2} - 1 \right)$$

$$\begin{aligned}
&= \left( \sqrt{R_1^2 - r^2} + \sqrt{R_2^2 - r^2} \right) \frac{1}{\lambda_1} \left( \frac{\lambda_1}{\lambda_2} - 1 \right) \\
\stackrel{\text{Taylor}}{\approx} &\left( R_1 - \frac{1}{2} \frac{r^2}{R_1} + R_2 - \frac{1}{2} \frac{r^2}{R_2} \right) \frac{1}{\lambda_1} \left( \frac{\lambda_1}{\lambda_2} - 1 \right) \\
&= \left( R_1 + R_2 - \frac{1}{2} r^2 \left( \frac{1}{R_1} + \frac{1}{R_2} \right) \right) \frac{1}{\lambda_1} \left( \frac{\lambda_1}{\lambda_2} - 1 \right)
\end{aligned}$$

This shows that the principal part of the phase shift is

$$\begin{aligned}
\varphi(r) &= -\frac{1}{2} \frac{r^2}{f} \frac{1}{\lambda_1}, \\
\text{where } \frac{1}{f} &= \left( \frac{\lambda_1}{\lambda_2} - 1 \right) \left( \frac{1}{R_1} + \frac{1}{R_2} \right).
\end{aligned}$$

Furthermore, we define  $k$  to be

$$k = \frac{2\pi}{\lambda_1}.$$

Thus, the ansatz (30) leads to

$$\begin{aligned}
&\mathcal{A}_i \frac{1}{q_i + z} \exp \left( -ik \left( z + \frac{r^2}{2(q_i + z)} \right) \right) \Big|_{z=0} \\
&= \mathcal{A}_{i-1} \frac{1}{q_{i-1} + z} \exp \left( -ik \left( z + \frac{r^2}{2(q_{i-1} + z)} \right) \right) \\
&\quad \cdot \exp \left( -2\pi i \left( -\frac{1}{2} \frac{r^2}{f} \frac{1}{\lambda_1} \right) \right) \Big|_{z=0} \\
&\Downarrow \\
&k \frac{1}{q_i} = k \frac{1}{q_{i-1}} - 2\pi \frac{1}{f} \frac{1}{\lambda_1} \\
&\text{and } \frac{\mathcal{A}_i}{q_i} = \frac{\mathcal{A}_{i-1}}{q_{i-1}} \\
&\Downarrow \\
&\frac{1}{q_i} = \frac{1}{q_{i-1}} - \frac{1}{f} \\
&\text{and } \mathcal{A}_i = \mathcal{A}_{i-1} \frac{q_i}{q_{i-1}} \\
&\Downarrow
\end{aligned}$$

$$q_i = \frac{q_{i-1}}{-\frac{1}{f}q_{i-1} + 1}$$

and  $\mathcal{A}_i = \mathcal{A}_{i-1} \frac{1}{1 - \frac{1}{f}q_{i-1}}$

This shows

**Formula 4** (ABCD matrix of a lense).

$$\begin{pmatrix} A & B \\ C & D \end{pmatrix} = \begin{pmatrix} 1 & 0 \\ -\frac{1}{f} & 1 \end{pmatrix} \quad \text{and} \quad \mathcal{A}_i = \mathcal{A}_{i-1} \frac{1}{1 - \frac{1}{f}q_{i-1}}$$

Observe that this formula preserves energy, since

$$\frac{|\mathcal{A}_i|}{|\text{Im}(q_i)|} = \frac{|\mathcal{A}_{i-1}|}{|\text{Im}(q_{i-1})|}.$$

(Show this by a calculation as a homework.)

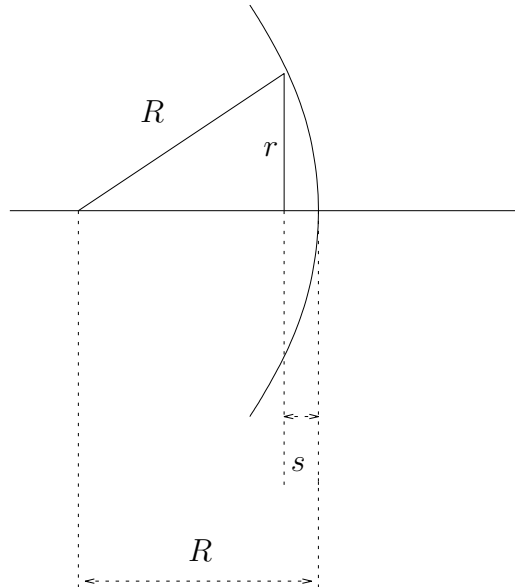


Figure 18: Phase shift of a mirror.

### 7.1.6 ABCD Matrix of a Mirror

Let us shift the mirror such that  $z_{i-1} = z_i = 0$ . The mirror leads to a phase shift

$$\exp(-ik(2s(r)))$$

where  $r = \sqrt{x^2 + y^2}$  such that

$$E_{i-1}(x, y, z) = E_i(x, y, z) \exp(+ik(2s(r))/\lambda) \quad (30)$$

Here we assume that the wave propagates before and after the mirror in the  $+z$  direction.

Let us first calculate this phase shift. By Figure 18, we see that

$$s(r) = R - \sqrt{R^2 - r^2} \stackrel{\text{Taylor}}{\approx} R - \left( R^2 - \frac{1}{2} \frac{r^2}{R} \right) = \frac{1}{2} \frac{r^2}{R}$$

Thus, we get

$$-ik \frac{r^2}{2(q_{i-1} + z)} = -ik \left( \frac{r^2}{R} + \frac{r^2}{2(q_i + z)} \right)$$

This implies

$$q_i = \frac{q_i + 0}{-q_{i-1} \frac{2}{R} + 1}$$

**Formula 5** (ABCD Matrix of a mirror).

$$\begin{pmatrix} A & B \\ C & D \end{pmatrix} = \begin{pmatrix} 1 & 0 \\ -\frac{2}{R} & 1 \end{pmatrix}$$

### 7.1.7 Other ABCD Matrices

The last two sections showed how to calculate the ABCD matrix of a lense and of free space. Similar calculations lead to the ABCD matrices of other apertures (see [2]). Here, additionally, let us mention the ABCD matrix of a ‘‘Gaussian Duct’’:

**Formula 6** (ABCD Matrix of a Duct).

Let  $k = \omega \sqrt{\mu \epsilon} n(x)$ , where  $n(x) = n_0 - \frac{1}{2} n_2 x^2$ . Then

$$\begin{pmatrix} A & B \\ C & D \end{pmatrix} = \begin{pmatrix} \cos(\gamma z) & (n_0 \gamma)^{-1} \sin(\gamma z) \\ -(n_0 \gamma) \sin(\gamma z) & \cos(\gamma z) \end{pmatrix},$$

where  $\gamma^2 = n_2/n_0$ .

### 7.1.8 Ray (or Beam) Matrix of the Resonator

The last sections showed how to calculate the ABCD matrix of a lense, mirror and free space.

Using the ABCD matrix  $M_i$  of each aperture on can calculate the ABCD matrix of the whole resonator by (see Lemma 2)

$$M = \prod_{i=1}^n M_i =: \begin{pmatrix} A & B \\ C & D \end{pmatrix}$$

**Lemma 3.**

$$\det \begin{pmatrix} A & B \\ C & D \end{pmatrix} = \det(M) = 1$$

*Proof.* Observe that for every aperture the corresponding ABCD matrix  $M_i$  satisfies  $\det(M_i) = 1$ .  $\square$

Let  $r_0$  be a start vector. Consider

$$r_s = M^s r_0$$

The eigenvalues of  $M$  are

$$\lambda_{a,b} := m_{\pm} \sqrt{m^2 - 1}, \quad \text{where } m = \frac{A+D}{2}.$$

Observe that  $\lambda_a \lambda_b = 1$ .

Let  $q_a, q_b$  be the eigenvectors of  $M$ . Decompose

$$r_0 = c_a q_a + c_b q_b.$$

Such a decomposition is possible, if  $q_a \neq q_b$ . This is the case of  $m \neq 1$ .

Then,

$$r_s = c_a \lambda_a^s q_a + c_b \lambda_b^s q_b.$$

- Stable Laser:  $-1 \leq |m| \leq 1$ . Then,

$$r_s = e^{i\Theta n} c_a q_a + e^{-i\Theta n} c_b q_b,$$

where  $\lambda_{a,b} := \cos \Theta \pm i \sin \Theta = e^{\pm i\Theta}$ .

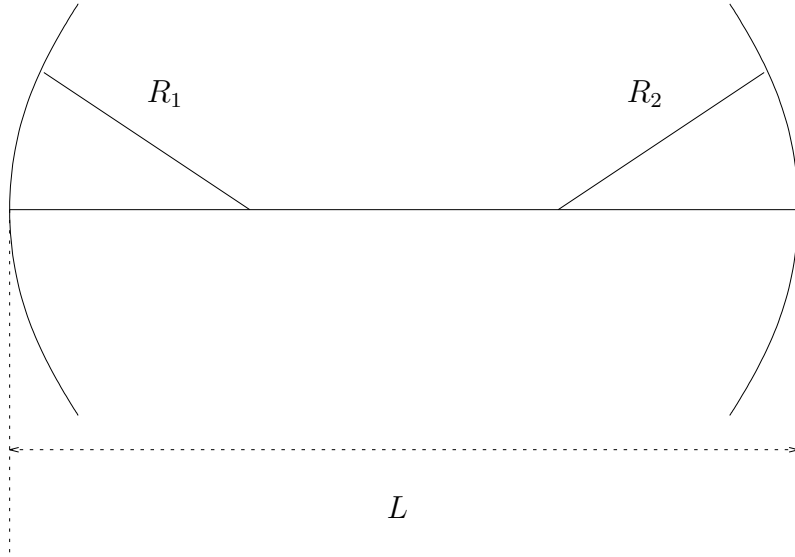


Figure 19: Example of a two mirror resonator.

- Unstable Laser:  $|m| \geq 1$ . Then,

$$r_s = M^s c_a q_a + M^{-s} c_b q_b,$$

where  $M = \lambda_a$ ,  $\frac{1}{M} = \lambda_b$ ,  $M = m + \sqrt{m^2 - 1}$ .

**Example 7** (Two Mirrors). *Let us assume  $n_0 = 0$ . Consider the resonator in Figure 19 with two mirrors and free space. The corresponding ABCD matrix for  $R_1 = R_2 = R$  is:*

$$M = \left( \left( \begin{array}{cc} 1 & 0 \\ -\frac{2}{R} & 1 \end{array} \right) \left( \begin{array}{cc} 1 & L \\ 0 & 1 \end{array} \right) \right)^2 = \left( \begin{array}{cc} 1 - \frac{2L}{R} & * \\ * & -\frac{2L}{R} + \left(1 - \frac{2L}{R}\right)^2 \end{array} \right)$$

Let us abbreviate  $m = \frac{A+D}{2}$  and  $\alpha = \frac{2L}{R}$ . Then,

$$m = 1 - 2\alpha + \frac{1}{2}\alpha^2.$$

Thus the resonator is stable ( $|M| \leq 1$ ) if and only if  $0 \leq \alpha \leq 4$ . This means

$$2R \geq L.$$





Figure 20: Gaussian duct.

### 7.1.9 Exact Solution in a Gaussian “Duct”

The refractive index of a Gaussian duct is (see Figure 20):

$$k = k_0 \left(1 - \frac{1}{2} n_2 r^2\right)$$

The paraxial approximation and neglecting the small high order term  $\frac{1}{4} n_2^2 r^2$  leads to

$$\Delta_{xy} \Psi - 2ik_0 \frac{\partial \Psi}{\partial z} - k_0^2 n_2 r^2 \Psi = 0$$

An exact solution of this equation is:

$$\Psi(x, y, z) = \exp \left( -\frac{x^2 + y^2}{w_1^2} + i \frac{\lambda z}{\pi w_1^2} \right)$$

where  $w_1^2 = 2 \frac{1}{k_0 \sqrt{n_2}}$  and  $\lambda = \frac{2\pi}{k_0}$ . Observe that  $\frac{\lambda z}{\pi w_1^2} = \sqrt{n_2} z$ .

### 7.1.10 The Guoy Phase Shift

Let us define the Guoy phase shift  $\psi(z)$  by:

$$\frac{i|q(z)|}{q(z)} = \exp(i\psi(z)).$$

This implies

$$\tan \psi(z) = \frac{\pi w(z)^2}{R(z)\lambda}.$$

Thus,  $\psi(z) = 0$  at the waist of the Gaussian beam.  
Then, one can show

$$\frac{1}{w_0} \frac{q_0}{q(z)} = \frac{\exp(i(\psi(z) - \psi_0))}{w(z)},$$

where  $\psi_0 = \psi(0)$  and  $q_0 = q(0)$ .

### 7.1.11 High Order Modes

Let us the notation in [4]:

In this book the spot size at the waist  $z = 0$  is:

$$w_D^2(z) = w_0^2 \left( 1 + \left( \frac{\lambda z}{\pi w_0^2} \right)^2 \right)$$

By (27), we get

$$\begin{aligned} w_D^2(z) = w(z) \Big|_{\text{Re}(q_0)=0} &= \frac{\lambda}{\pi} \left( \text{Im}(q_0) + \frac{(\text{Re}(q_0) + z)^2}{\text{Im}(q_0)} \right) \Big|_{\text{Re}(q_0)=0} \\ &\Rightarrow w_0^2 = \frac{\lambda}{\pi} \text{Im}(q_0) \end{aligned}$$

and

$$R(z) = (\text{Re}(q_0) + z) \left( 1 + \frac{\text{Im}(q_0)^2}{(\text{Re}(q_0) + z)^2} \right)^2$$

#### Hermite-Gaussian Modes

By this notation, we get the Hermite-Gaussian Modes:

$$\begin{aligned} \Psi_{m,n} &= \frac{w_0}{w} H_m \left( \sqrt{2} \frac{x}{w} \right) H_n \left( \sqrt{2} \frac{y}{w} \right) \\ &\quad \exp \left( -i(kz - \Phi) - r^2 \left( \frac{1}{w^2} + \frac{ik}{2R} \right) \right) \end{aligned}$$

where

$$\begin{aligned} \Phi(m, n, z) &= (m + n + 1) \tan^{-1} \left( \frac{\lambda z}{\pi w_0^2} \right) \\ H_0(x) &= 1, & H_1(x) &= x, \\ H_2(x) &= 4x^2 - 2, \dots \\ H_n(x) &= (-1)^n e^{x^2} \frac{d^n}{dx^n} (e^{-x^2}) & n &= 0, 1, \dots \end{aligned}$$

The set of these functions forms a basis.

#### Laguerre-Gaussian Modes

The absolute value of the Laguerre-Gaussian Mode  $\Psi_{m,n}$  is:

$$|\Psi_{m,n}| = E_0 \left( \sqrt{2} \frac{r}{w_D} \right)^l L_p^l \left( 2 \frac{r^2}{w_D^2} \right) e^{-\frac{r^2}{w_D^2}} \cos(l\phi)$$

where  $r, \phi$  are the angle coordinates and

$$\begin{aligned} L_0^l(x) &= 1 & L_1^l(x) &= l + 1 - x \\ L_2^l(x) &= \frac{1}{2}(l+1)(l+2) - (l+2)x + \frac{1}{2}x^2 \\ L_n(x) &= e^x \frac{d^n}{dx^n} (x^n e^{-x}) & n &= 0, 1, \dots \end{aligned}$$

The set of these functions forms a basis.

#### 7.1.12 Thermal Lensing

The refraction index  $n_c(x)$  of a laser crystal changes by

- a) thermal lensing .
  - b) internal change of the refraction index caused by deformation
  - c) deformation of the end faces of the laser crystal
- a) The refraction index of a laser crystal changes by temperature
- Let  $T_0$  be the temperature before heating (refraction index  $n_0$ ).
  - Let  $T$  be the temperature caused by the pumping process (refraction index  $n$ ).

Let  $\eta_T$  be the thermal index gradient.

(Example:  $\eta_T = 2.2 \cdot 10^{-6} \cdot \text{ }^\circ\text{C}^{-1}$  for  $\text{Cr}^{4+}$ ).

Then,

$$n(x, y, z) = n_0 + \eta_T(T(x, y, z) - T_0)$$

The heating of the laser crystal leads to a deformation of the laser crystal. This deformation can be described in the following way.

Let  $\mathcal{B} \subset \mathbb{R}^3$  be the original domain of the laser crystal.  
Let  $T : \mathcal{B} \rightarrow \mathbb{R}^3$  be the mapping of the laser deformation such that

$$\{T(x) + x \mid x \in \mathcal{B}\}$$

is the deformed domain of the laser crystal.

- Heat and
- deformation

of the crystal lead to a refraction index

$$n_c(x), \quad x \in \mathcal{B}$$

such that  $k_c(x) = \omega \sqrt{\mu \epsilon} n_c(x)$ .

Assume that  $\mathcal{B} = \mathcal{D} \times ]0, L[$ ,  $L$  length of the laser crystal.

b) The parabolic fit of the refraction index is

- Subdivide  $]0, L[$  in  $N$  intervals of meshsize  $h = \frac{L}{N}$ .
- Let  $\mathcal{D}_h$  be the discretization grid.
- For every  $i = 0, \dots, N - 1$ : Find  $n_{0,i}, n_{2,i}$  such that:

$$\left\| n_c(x, y, h(i + \frac{1}{2})) - (n_{0,i} - \frac{1}{2}n_{2,i}(x^2 + y^2)) \right\|_{l^2(\mathcal{D}_h)}$$

- Each of the parameters  $n_{0,i}, n_{2,i}$  lead to a matrix

$$A_i = \begin{bmatrix} \cos \gamma_i z & n_0 \gamma_i^{-1} \sin \gamma_i z \\ n_0 \gamma_i \sin \gamma_i z & \cos \gamma_i z \end{bmatrix}$$

c) Additionally, perform a parabolic fit of  $T(x, y, 0)$  and  $T(x, y, L)$ .

## 7.2 Iteration Method of Fox and Li

The iteration method of Fox and Li applies the beam propagation method.

Consider a resonator with a left and right mirror. Let  $\Psi^{\text{initial}}$  be an initial condition at the left mirror. By the BMethod calculate

- the beam configuration at the right mirror and the
- reflected beam configuration  $\Psi^{\text{end}} := \mathcal{B}(\Psi^{\text{initial}})$  at the left mirror.

If  $\Psi^{\text{initial}} = \Psi^{\text{end}}$ , then  $\Psi^{\text{initial}}$  is an eigenvector  $\Psi^{\text{eigen}}$  of the BPM operator  $\mathcal{B}$ .

The iteration method of Fox and Li is a power iteration method for the eigenvalue problem of the BPM operator  $\mathcal{B}$ .

This means:

$$\begin{aligned} \Psi^1 &= \Psi^{\text{initial}}, & \Psi^{s+1} &= \mathcal{B}(\Psi^{\text{initial},s}) \\ \Psi^{\text{eigen}} &= \lim_{s \rightarrow \infty} \Psi^s \end{aligned}$$

The advantages of the BPM and Fox and Li method are:

- 3D approximation
- more general
- simple method

The disadvantages of the BPM and Fox and Li method are:

- no or bad convergence due to several eigenvectors with eigenvalues close to each other.
- bad convergence due to round off errors
- low accuracy
- large computational time
- model errors by the paraxial approximation

## 8 Finite Element Discretization of Optical Waves in Semiconductor Laser Resonators

### 8.1 Construction of Semiconductor Lasers

Semiconductors have different physical properties than solid materials. One of them is that the energy bands in semiconductors are not discrete but a

band. To select certain frequencies, most diode lasers use gratings or distributed Bragg reflectors (DBR). A VCSEL (Vertical Cavity Surface Emitting Laser) is depicted in Figure 21 and a DFB laser (Distributed Feedback Laser) in Figure 22.

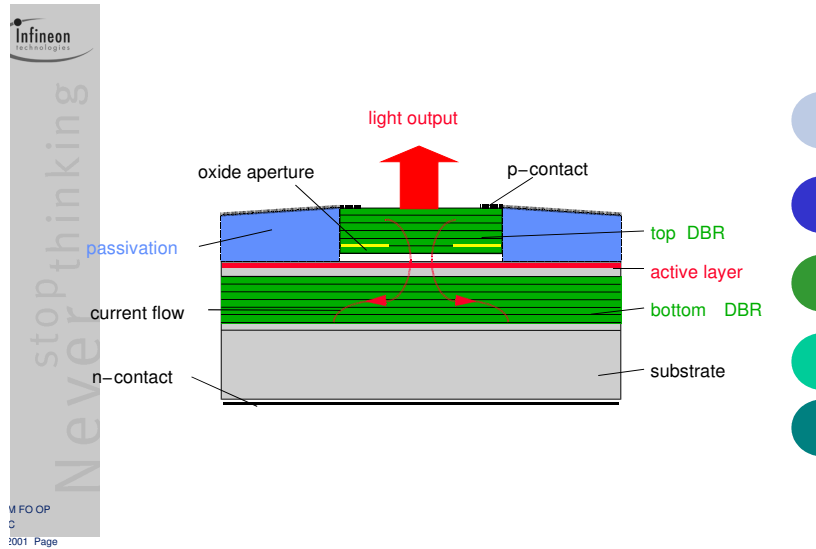


Figure 21: VCSEL (Vertical Cavity Surface Emitting Laser)

## 8.2 Transfer Matrix Method

To obtain a gain of light for a certain frequency several different constructions are used. The main concept is to use layers of materials with different refraction indices. These layers of different materials form the resonators.

Let us assume that the resonator has the form

$$\Omega = \Psi \times [0, L]$$

and that  $0 = l_0 < l_1 < \dots < l_s = L$  Furthermore, let us assume that the resonator has the refraction index  $n_i$  ( $k_i$ ) in the layer  $\Psi \times [l_{i-1}, l_i]$ . Since the layers are very thin, it is important to take into account reflection at the interfaces of the different materials. To understand this in more detail let us consider the 1D case. Assume that

$$-E'' - k^2 E = 0.$$

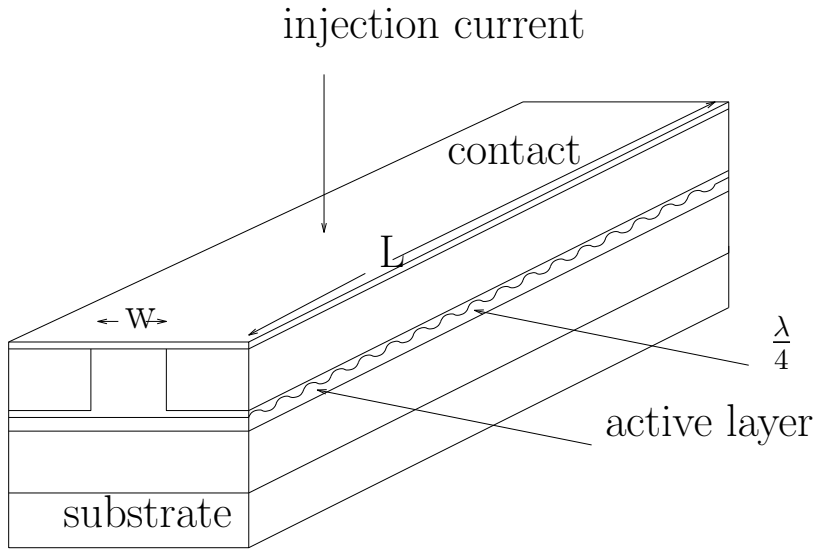


Figure 22: VCSEL (Distributed Feedback Laser)

Let us assume the  $k$  is constant in the interior of  $[l_{i-1}, l_i]$ . Then,

$$E(z) = c_{i,r} \exp(-ik_i(z - l_{i-1})) + c_{i,l} \exp(ik_i(z - l_{i-1})) \quad \text{for } z \in [l_{i-1}, l_i].$$

By the regularity of differential equations, we obtain  $E \in C^1([0, L])$ . This leads to the following equations at the interfaces (see Figure 23):

$$\begin{aligned}
c_{i,r} \exp(-ik_i(l_i - l_{i-1})) + c_{i,l} \exp(ik_i(l_i - l_{i-1})) &= c_{i+1,r} + c_{i+1,l} \\
-c_{i,r} \exp(-ik_i(l_i - l_{i-1}))k_i + c_{i,l} \exp(ik_i(l_i - l_{i-1}))k_i &= (-c_{i+1,r}k_{i+1} + c_{i+1,l}k_{i+1}).
\end{aligned}$$

Let us abbreviate  $h_i = l_i - l_{i-1}$ . Then, we get

$$\begin{aligned}
& \begin{pmatrix} 1 & 1 \\ -k_i & k_i \end{pmatrix} \begin{pmatrix} \exp(-ik_i h_i) & 0 \\ 0 & \exp(ik_i h_i) \end{pmatrix} \begin{pmatrix} c_{i,r} \\ c_{i,l} \end{pmatrix} \\
&= \begin{pmatrix} 1 & 1 \\ -k_{i+1} & k_{i+1} \end{pmatrix} \begin{pmatrix} c_{i+1,r} \\ c_{i+1,l} \end{pmatrix} \\
&\Downarrow \\
& \begin{pmatrix} c_{i+1,r} \\ c_{i+1,l} \end{pmatrix} = M_i \begin{pmatrix} c_{i,r} \\ c_{i,l} \end{pmatrix} \\
M_i &= \begin{pmatrix} 1 & 1 \\ -k_{i+1} & k_{i+1} \end{pmatrix}^{-1} \\
& \begin{pmatrix} 1 & 1 \\ -k_i & k_i \end{pmatrix} \begin{pmatrix} \exp(-ik_i h_i) & 0 \\ 0 & \exp(ik_i h_i) \end{pmatrix} \\
M_i &= \begin{pmatrix} k_{i+1} + k_i & k_{i+1} - k_i \\ k_{i+1} - k_i & k_{i+1} + k_i \end{pmatrix} \cdot \frac{1}{2k_{i+1}} \begin{pmatrix} \exp(-ik_i h_i) & 0 \\ 0 & \exp(ik_i h_i) \end{pmatrix}.
\end{aligned}$$

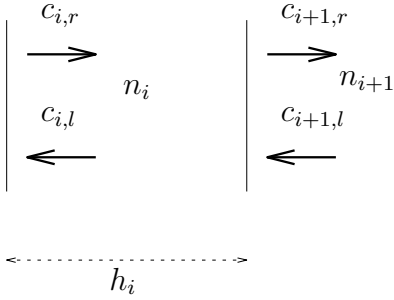


Figure 23: Transmission of two waves from one layer to another layer

In general one can describe the behavior by a scattering matrix  $S$  and a transmission matrix  $T$ :

$$\begin{pmatrix} c_{1,r} \\ c_{1,l} \end{pmatrix} = T \begin{pmatrix} c_{2,r} \\ c_{2,l} \end{pmatrix} \quad \begin{pmatrix} c_{2,r} \\ c_{1,l} \end{pmatrix} = S \begin{pmatrix} c_{1,r} \\ c_{2,l} \end{pmatrix}$$



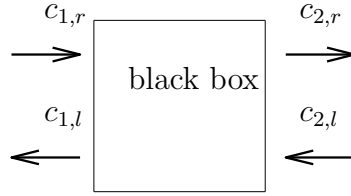


Figure 24: Black box

**Example 8.** Let us study 101 layers with refraction index  $n_0, n_1, n_0, \dots, n_0$ ,  $\lambda_0 = 1.6 \cdot 10^{-6}$ ,  $k_0 = \frac{2\pi}{\lambda_0}$ , and  $\omega = \frac{k}{\sqrt{\epsilon_0 \mu_0 n_0}}$ , where  $\sqrt{\epsilon_0 \mu_0} = \frac{1}{c}$  and  $n_0 = 3.277$ . Let us choose  $c_{2,l} = 1$ ,  $c_{1,r} = 0$ . Then,  $c_{1,l}$  shows the behavior of the construction. Figure 25 and Figure 26 depict  $c_{1,l}$  with respect to  $\omega$ .

A high reflectivity is obtained for  $\omega = \omega_0, 3\omega_0, 5\omega_0, \dots$

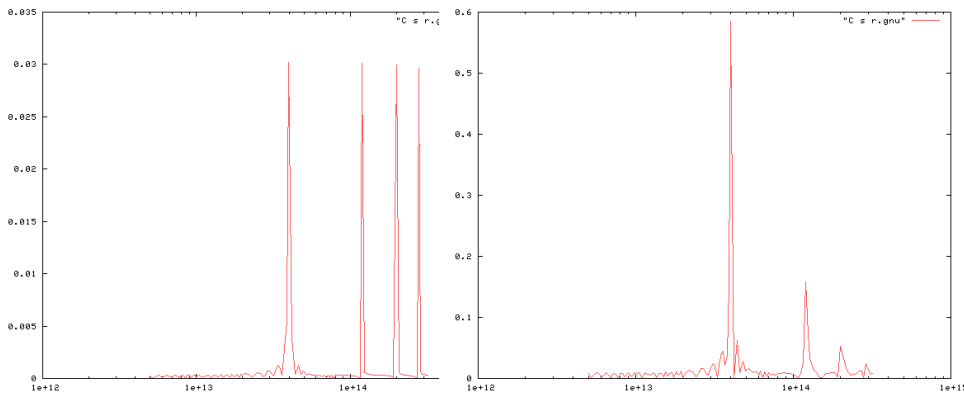


Figure 25: Reflection behavior for  $n_1 = 3.275$ .

Figure 26: Reflection behavior for  $n_1 = 3.220$ .

## References

- [1] A. Taflove and S. Hagness. *Computational Electrodynamics: The Finite-Difference Time-Domain Method*. Artech House, Boston, London, 2000.
- [2] Siegman. *Lasers*. University Science Books Sausalito, California.
- [3] R. Kröger and R. Unbehauen. *Technische Elektrodynamik*. Teubner Stuttgart, 1987.
- [4] Christopher C. Davis. *Lasers and Electro-Optics (Fundamentals and Engineering)* Cambridge University Press.
- [5] Coldren and Corzine *Diode Lasers and Photonic Integrated Circuits* Wiley
- [6] Amnon Yariv. *Introduction to Optical Electronics*.
- [7] Amnon Yariv. *Optical Waves in Crystals*.
- [8] Koechner. *Solid-State Laser Engineering*.
- [9] Hecht. *Optik*.
- [10] Braess. *Finite Elemente* Springer.
- [11] Ihlenburg. *Finite Element Analysis of Acoustic Scattering*. Springer.
- [12] Jianming Jin. *The Finite Element Method in Electromagnetics*. John Wiley & Sons.
- [13] Altmann, Pflaum, Seider. *3D Finite Element Computation of Laser Cavity Eigenmodes*. Applied Optics-LPE . vol. 43, issue 9, page 1892, 2004.
- [14] F. Ihlenburg. *Finite Element Analysis of Acoustic Scattering*, volume 132 of *Springer Series Applied Mathematical Sciences*. Springer, New York, Paris, London, 1998.